

Northumbria Research Link

Citation: Kahlert, Thorsten, O'Donnell, Shawn, Stimpson, Christopher, Mai Hương, Nguyễn Thị, Hill, Evan, Utting, Benjamin and Rabett, Ryan (2021) Mid-Holocene coastline reconstruction from geomorphological sea level indicators in the Tràng An World Heritage Site, Northern Vietnam. *Quaternary Science Reviews*, 263. p. 107001. ISSN 0277-3791

Published by: Elsevier

URL: <https://doi.org/10.1016/j.quascirev.2021.107001>
<<https://doi.org/10.1016/j.quascirev.2021.107001>>

This version was downloaded from Northumbria Research Link:
<http://nrl.northumbria.ac.uk/id/eprint/47927/>

Northumbria University has developed Northumbria Research Link (NRL) to enable users to access the University's research output. Copyright © and moral rights for items on NRL are retained by the individual author(s) and/or other copyright owners. Single copies of full items can be reproduced, displayed or performed, and given to third parties in any format or medium for personal research or study, educational, or not-for-profit purposes without prior permission or charge, provided the authors, title and full bibliographic details are given, as well as a hyperlink and/or URL to the original metadata page. The content must not be changed in any way. Full items must not be sold commercially in any format or medium without formal permission of the copyright holder. The full policy is available online: <http://nrl.northumbria.ac.uk/policies.html>

This document may differ from the final, published version of the research and has been made available online in accordance with publisher policies. To read and/or cite from the published version of the research, please visit the publisher's website (a subscription may be required.)

1 **Title**

2 Mid-Holocene coastline reconstruction from geomorphological sea level indicators in the
3 Tràng An World Heritage Site, Northern Vietnam

4

5 **Author names and affiliations**

6 ¹Thorsten Kahlert, ¹Shawn O'Donnell, ¹Christopher Stimpson, ^{1,2}Nguyễn Thị Mai Hương,

7 ¹Evan Hill, ³Benjamin Utting, ¹Ryan Rabett

8

9 ¹School of Natural & Built Environment, Queen's University Belfast, Elmwood Avenue,
10 Belfast BT7 1NN, UK

11 ²Vietnam Academy of Social Sciences, Institute of Archaeology, 61 Phan Chu Trinh Str.,
12 Hoan Kiem, Hanoi, Vietnam.

13 ³ Department of Archaeology, University of Cambridge, Downing Street, Cambridge CB2
14 3DZ, UK.

15

16 **Corresponding author**

17 Thorsten Kahlert, School of Natural and Built Environment, Queen's University
18 Belfast, University Road, Belfast BT7 1NN, Northern Ireland, United Kingdom

19 t.kahlert@qub.ac.uk

20

21 **Tables: 5, References: 105**

22 **Figures (18 total):**

23 **Single column: 10, 11, 12, 14, 16 Double column: 1, 2, 3, 4, 5, 6, 7, 8, 9, 13, 15, 17, 18**

24 **Recommended colour print: 5, 6, 9, 17, 18**

25 **Abstract**

26 In this paper we present a high resolution palaeo coastline model for the isolated limestone
27 massif of Trảng An, Ninh Bình province, Vietnam. The archaeological and palaeoecological
28 record here comprise rich archives of human activity set within a landscape that was
29 cyclically transformed between inland and archipelagic states under the influence of past sea
30 level changes. These records have become informative proxies in the study of current sea
31 level rise. Well-preserved notches along the vertical limestone cliffs within the study property
32 reveal several phases of prolonged stable sea levels that likely pertain to the Mid-Holocene
33 marine transgression 8 ka BP to 4 ka BP and allow for detailed coastline reconstructions for
34 parts of the Red River Delta (RRD). The resulting coastline model facilitates a closer look at
35 past human responses to landscape and environmental changes at local and individual site-
36 level, which improves our understanding of past human adaptations to climate-change
37 induced sea level rise. These data also stand to inform current coastal vulnerability
38 assessments and climate change response models.

39

40 **Keywords**

41 Holocene; Pleistocene; Climate dynamics; Sea Level changes; Southeast Asia;
42 Geomorphology, coastal; Data treatment, data analysis

43

44 **1. Introduction**

45 More than 23% of the world's population live on the coast; a figure heavily weighted towards
46 populations in South, Southeast and East Asia (Small and Nicholls, 2003). Coastal
47 communities in this part of the world are facing an urgent threat from above-average climate-
48 driven sea level rise (Nicholls and Cazenave, 2010; Hens et al., 2018). Global and regional

49 models are now seeking to assess future coastal vulnerability in increasingly complex ways.
50 This has included a drive towards incorporating natural and social science data into economic
51 integrated assessment models. The Dynamic and Interactive Vulnerability Assessment
52 (DIVA) tool (Hinkel, 2005), has found particular utility across a range of models at different
53 scales (e.g. Vafeidis et al., 2008; Hinkel et al., 2010; Brown et al., 2016; Diaz, 2016; Muis et
54 al., 2017; Tamura et al., 2019). Equally fundamental to impact projections is an
55 understanding of changes in relative sea level, geological processes and punctuated extreme
56 events (e.g. tsunami or storms). The study of these variables and their effects on coastal areas,
57 people and biodiversity have been the subject of several initiatives sponsored by the
58 International Geoscience Programme (formerly the International Geoscience Correlation
59 Programme (IGCP) since the 1970s, including the recent projects IGCP437 (1999 – 2003)
60 ‘Coastal environmental change during sea-level highstands: a global synthesis with
61 implications for management of future coastal changes’ (Murray-Wallace et al., 2003) and
62 IGCP588 (2010 – 2014) and ‘Preparing for Coastal Change’ (Sloss et al., 2012).
63 Palaeoenvironmental data, such as that provided by sedimentary sequences, relic coral reefs
64 and notches also have a significant contribution to make by providing detailed records of how
65 sea levels have changed in the past, where shorelines lay and how coastal settings previously
66 responded to these changes (e.g. Liew et al., 1993; Hanebuth et al., 2000; Wang et al., 2008;
67 Murray-Wallace and Woodroffe, 2014; Kelsey, 2015). In Southeast Asia,
68 palaeoenvironmental proxies have been used to track inundation of the Sunda and adjacent
69 continental shelves after the Last Glacial Maximum (LGM: 26 – 18 ka BP), which not only
70 submerged more than 1.8 million km² between Indonesia and Vietnam but reshaped
71 coastlines and entire river and deltaic systems (Hanebuth et al., 2000; Hanebuth et al., 2009;
72 Rabett and Jones, 2014).

73 Past coastal inundations driven by rising sea level contributed to dramatic changes to coastal
74 landscapes, particularly in river deltas where low-gradient flood plains were inundated for
75 hundreds of kilometres, triggering changes in habitats, biodiversity and human culture over
76 prolonged periods of time (Stanley and Warne, 1994; Stanley and Warne, 1997). Sediment
77 cores, geomorphological sea level markers, alongside archaeological and historical records,
78 are used to develop coastline models that satisfy a general understanding of the impact of sea
79 level changes on coastal landscapes at regional and global scales (Pirazzoli, 1991). While
80 such models can inform models of past cultural adaptation and environmental changes, and in
81 a broader sense what triggers them, they provide insufficient detail to study these
82 mechanisms at local and site levels. Palaeoenvironmental samples from sediment cores and
83 archaeological sites are of limited spatial extent, and their formation is determined by the
84 immediate conditions that surround a site. As such, detailed coastal models of geographically
85 limited extent improve the overall understanding of the conditions at a site at a specific point
86 in time and remove uncertainties surrounding site formation processes (e.g. Surakiatchai et
87 al., 2018; O'Donnell et al., 2020). Feedback from these punctuated studies can then be
88 applied to large-scale coastal reconstructions to improve their overall accuracy.

89 In this paper we present a relative time-series coastline reconstruction and distribution maps
90 for part of the Red River Delta (RRD) in northern Vietnam during the Mid-Holocene sea
91 transgression. Our model is based on a survey of 27 notches all taken within an isolated karst
92 massif within the RRD, which act as indicators for past relative sea levels (here, rsl pertains
93 to past topographic conditions relative to modern elevation above sea level, not adjusted for
94 isostatic and eustatic changes (Rovere et al., 2016). In particular, we illustrate how variations
95 in sea level at the metre-scale have impacted this topographically complex landscape,
96 providing detailed landscape-scale spatial evidence to reconstruct past human activity and
97 ecosystem development in this part of the RRD. Our data also exemplify the detail that can

98 be lost to current assessment models of contemporary coastal vulnerability when spatial
99 structuring and time-depth dimensions are not considered. At present, the lack of a high-
100 resolution chronology prevents immediate incorporation of our data into the regional sea
101 level curve (e.g. Hanebuth et al., 2011); however, this remains an achievable future aim.

102 *1.1 Notch formation*

103 During periods of eustatic sea level rise, isolated upland formations set in coastal alluvial
104 plains may become inundated and temporarily transformed into islands or archipelagos.

105 Under such conditions marine notches may form and their morphology indicates the extent
106 and duration of past marine transgressions along with local coastal conditions (Pirazzoli,
107 1986; Boyd and Lam, 2004; McDonald and Twidale, 2011; Moses, 2012; Trenhaile 2015).

108 Their use as eustatic sea level markers is accompanied by sometimes wide error margins and
109 uncertainty due to absence of direct dating material. Geological, geomorphological,
110 biological and marine factors that influence sea level estimations from notch morphology
111 (Woodroffe and Horton, 2005; Trenhaile 2014, 2015, 2016), however, can still be used
112 effectively in the reconstruction of local and regional rsl and coastlines (Surakiatchai et al.,
113 2018). Indeed, the development of notches plays an important role in the life-cycle of
114 lowland and coastal karst landscapes in tropical South and Southeast Asia (Scheffers et al.,
115 2012; Mann et al., 2019) and, where preserved, serve as excellent past rsl indicators
116 (Pirazzoli, 1986).

117 Notches considered in this study form in two principal environments: 1) marine notches,
118 which form within coastal littoral zones; 2) basal or swamp notches, which form along the
119 water table in freshwater or brackish environments. Used in conjunction with terrestrial and
120 marine sediment cores, and radiometric dating, the extent, composition and chronology of
121 palaeo-coastlines can be modelled, and then utilised in a variety of contexts including
122 reconstruction of past human activity and ecosystem development; refinement of local and

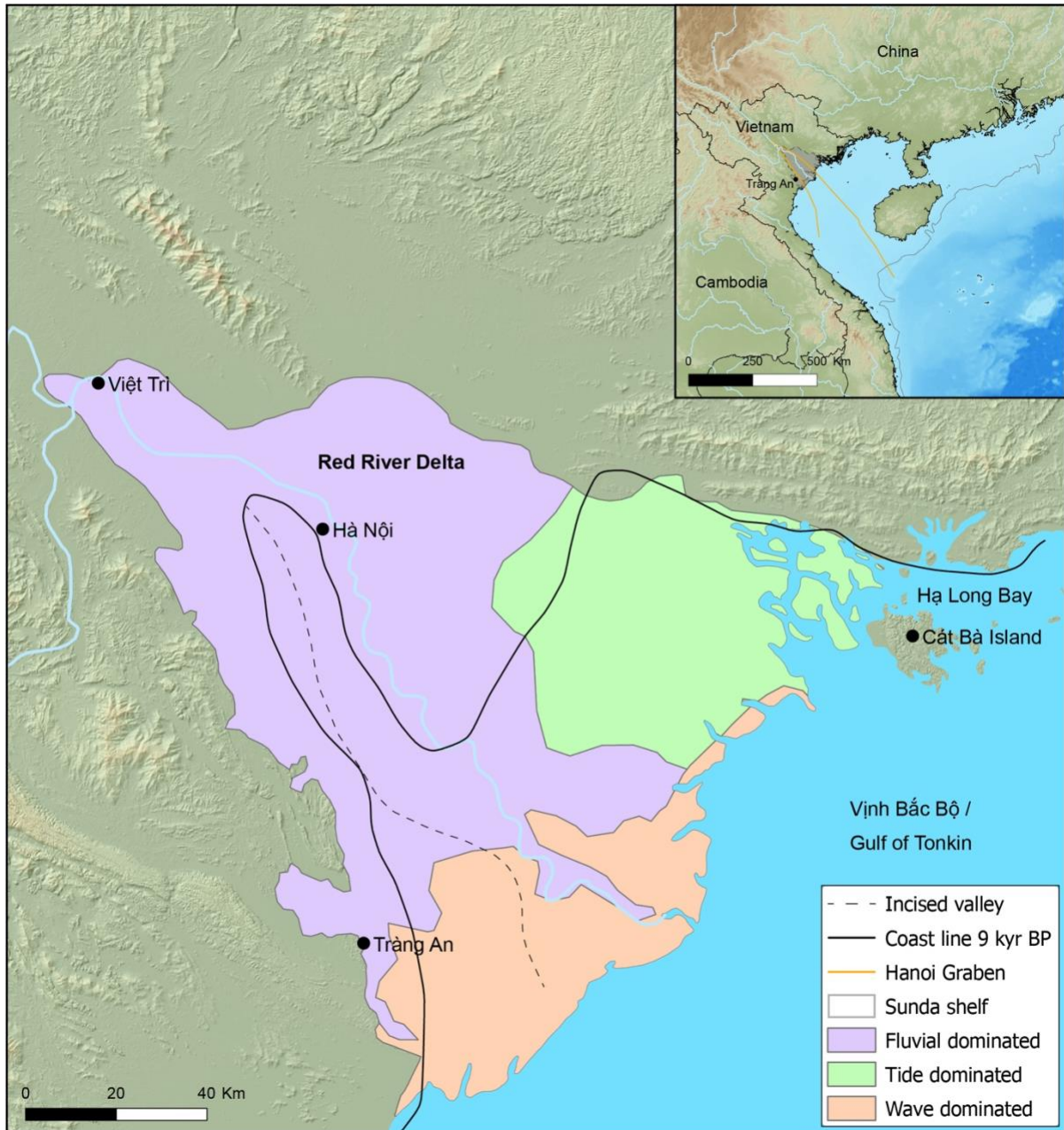
123 regional sea level curves; and development of risk mitigation strategies against future coastal
124 inundation (Liew et al., 1993; Hanebuth et al., 2000; Wang et al., 2008; Murray-Wallace and
125 Woodroffe, 2014; Kelsey, 2015).

126 Along the carbonate rock coasts of Vịnh Bắc Bộ (Gulf of Tonkin), the islands of Hạ Long
127 Bay/ Cát Bà and on the terrestrial southwestern margins of the RRD (Figure 1), well
128 preserved notches are reported at elevations ranging between 2 and 9 m above sea level (here,
129 asl pertains to elevation above modern sea level relative to a global geoid and/or local datum
130 such as EGM96) indicative of Quaternary sea levels that were at times above those of today
131 (Boyd and Lam, 2004; Pham et al., 2013). Radiometric dates obtained from material
132 recovered from notches in Hạ Long Bay and in the Tràng An massif (Figure 1) suggest that
133 the majority formed during the Mid-Holocene transgression between 6 and 3 ka BP (dates
134 quoted as ka BP = “thousands of years before present”, where “present” is 1950. Where
135 available, calibrated dates are shown with 2σ ranges, unless otherwise stated) (Boyd and
136 Lam, 2004; Tran et al., 2013). Post-6 ka BP transgressions were also proposed by Pedoja
137 (2008) - citing Xie et al. (1985) - and Zhang et al. (2003) at 5 ka BP and 3 ka BP, reaching 4
138 ± 1 m asl and 1.5 ± 1 m asl respectively for the South China Sea. Notches at 1.5 – 2 m asl have
139 been recorded in the RRD (Nguyen et al., 2012a; Pham et al., 2013; Tran et al., 2013), dated
140 to 2.5 – 1.5 ka BP, and interpreted as evidence for a Late-Holocene high stand.

141 Using deltaic sediments as past sea level markers poses challenges due to complex formation
142 processes such as erosion, reworking, bioturbation and compaction that cause highly
143 localised variability in lithological sequences and chronology (Mann et al., 2019). This can
144 lead to misinterpretation of results or loss of resolution in data. For example, evidence from
145 marine terraces, marine notches, corals, molluscs and crustacea has been observed across
146 Southeast Asia and attributed to a late Holocene high stand (Tjia, 1996; Baker and Haworth,
147 2000; Liew and Hsieh, 2000). Sequences covering the same period from three sediment cores

148 taken c. 30 – 50 km east and north of Trảng An lacked this evidence. Instead, a floodplain
149 environment with constantly decreasing sea level has been proposed until modern sea levels
150 were attained (Tanabe et al., 2003a; Tanabe et al., 2003b; Hori et al., 2004; Tanabe et al.,
151 2006).

152 In this paper, we expand the record of notches recorded in Trảng An (Boyd and Lam, 2004;
153 Nguyen et al., 2012a; Tran et al., 2013; UNESCO, 2014b) (Figure 1) to retrace the palaeo-
154 coast on the southwestern margin of the RRD. Using the work of Boyd and Lam (2004) as a
155 baseline, we examine the extent to which variable karst topography may be implicated in
156 altering tidal hydrology and therefore notch formation. We also propose minimum and
157 maximum Mid-Holocene coastlines for Trảng An, extending the transgression of the south-
158 western lower RRD further west than previously assumed (Tanabe et al., 2003b; Tanabe et
159 al., 2006; Tran et al., 2013), a finding that changes the current interpretation of the central
160 massif of Trảng An during that time from a peninsula to the largest island of a Trảng An
161 archipelago.



162

163 *Figure 1: Red River Delta divided into its three principal sedimentary zones overlain by the location of the incised valley*
 164 *and palaeo coastline at 9 ka BP (after Tanabe et al., 2006). Inset depicting location of RRD in its wider geographic context*
 165 *and Hanoi Graben (after Nielsen et al., 1999).*

166 *1.2 Geographic and geological setting*

167 Trảng An was inscribed as a mixed natural and cultural UNESCO World Heritage Site
 168 (WHS) in 2014, currently the only site in Southeast Asia to receive this status. This isolated
 169 limestone massif lies in the Province of Ninh Bình, immediately west of the provincial capital

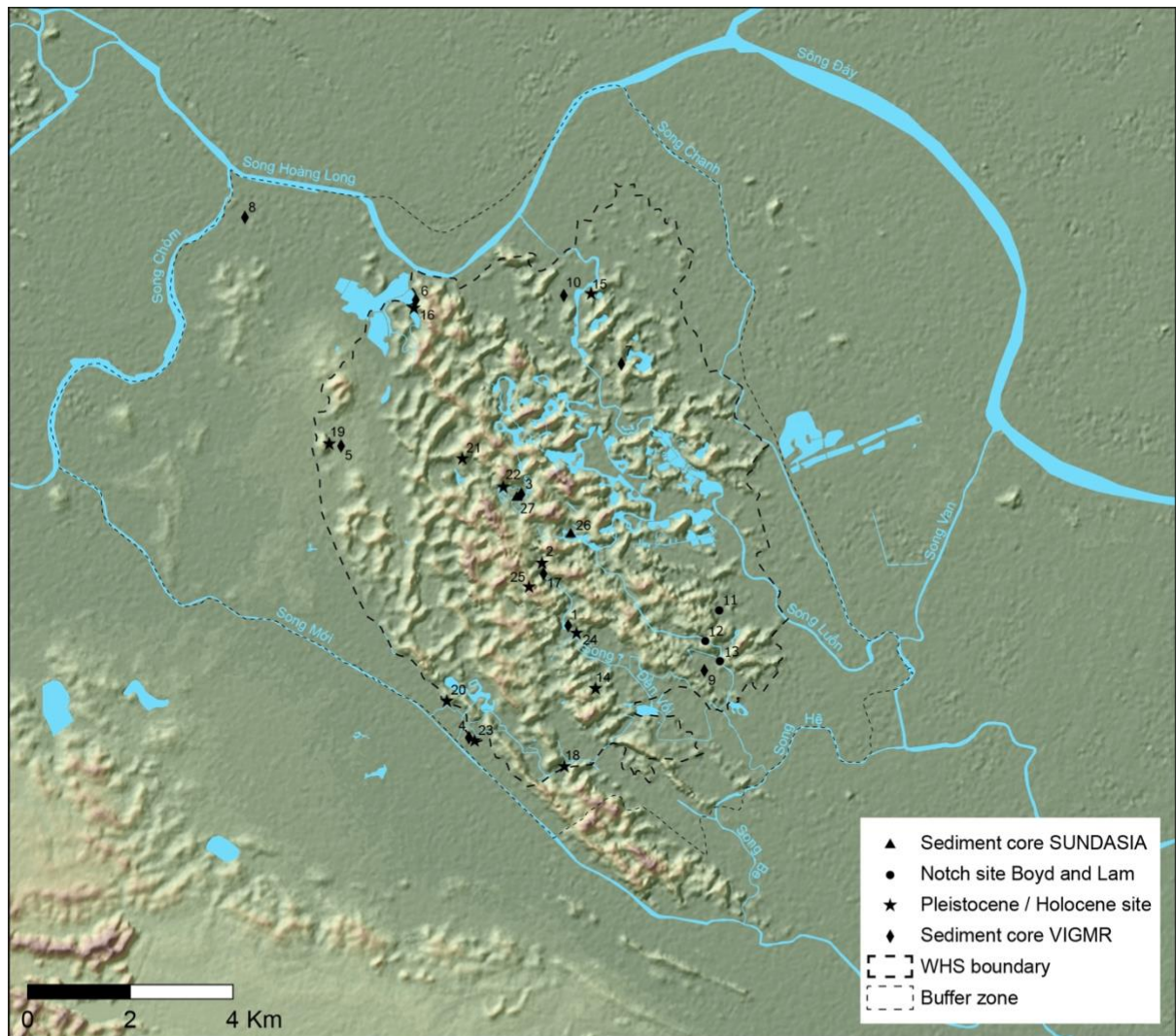
170 of the same name. The inscription marks Tràng An as an outstanding area of tropical
171 limestone karst with a human presence for the last 30 ka that illustrates adaptation to extreme
172 environmental changes (UNESCO, 2014b). The RRD itself extends c. 180 km northwest to
173 southeast and spans c. 150 km along the North Vietnam coast (Mathers et al., 1996; Mathers
174 and Zalasiewicz, 1999). The delta covers an area of c. 10,000 km² (Tanabe et al., 2003b) and
175 has a population density in excess of 430 persons/km², making it one of the most densely
176 populated river deltas in the region (Fanchette, 2002; Labbé, 2019). The delta has formed
177 within the seismically active Red River Graben, a major fault that divides the North Vietnam
178 and Sông Đà terranes. The Red River Graben is controlled by a complex of fault systems; the
179 southern-most of which being the Red River fault that also controls the course of the Sông
180 Đáy (Phach et al., 2020). The Red River Graben is filled with Neogene and Quaternary
181 sediments to a depth of up to 3 km and limited by Pre-Quaternary mountainous uplands
182 (Mathers et al., 1996). These deposits are overlain by alluvial and marine sediments laid
183 during delta initiation from c. 9 ka BP (Tanabe et al., 2003b) (see also Appendix A.1).
184 Surface topographical and geological studies indicate three sub-systems that influenced delta
185 morphology (Mathers and Zalasiewicz, 1999). The inland western section of the delta is
186 alluvial-dominated, the northern section is tide-dominated and the southern section is wave-
187 dominated (Figure 1). The Leizhou Peninsula and Hainan Island afford a degree of protection
188 for the northern coast to direct wave action contributing to the development of these
189 contrasting systems.

190 Situated c. 85 km south of Hanoi and 45 km west of the coast of Vịnh Bắc Bộ, the Tràng An
191 massif lies adjacent to the infilled Sông Hồng valley, an incised river valley that was
192 inundated after the LGM and had been infilled with tide-influenced channel sediments by 6
193 ka BP (Tanabe et al., 2003b). To its west, Tràng An is adjoined by an elevated Pleistocene
194 fluvial terrace that rises above the otherwise low-lying Holocene marine-influenced and

195 alluvial plains. The former is currently used to indicate the maximum extent of the Mid-
196 Holocene sea transgression (Tanabe et al., 2003b). Its full extent, however, has not yet been
197 established.

198 An interconnected river–canal system that has been intensely modified for transport and
199 irrigation flows through and around Tràng An, with the Sông Đáy being the largest river. To
200 the west, a 1 – 4 km wide poljie separates Tràng An from the eastern fringe of the Annamite
201 Mountains and forms a flood plain for the Sông Múi as it follows the western margin of the
202 Tràng An massif.

203 Previous investigations in Tràng An comprise studies that preceded the WHS inscription and
204 which included a series of sediment cores (see Appendix A.1), and geological,
205 geomorphological and archaeological assessments (UNESCO, 2014b). A limited notch
206 survey has also formed part of a broader project that investigated sea level changes in the
207 RRD (Lam and Boyd, 2001; Lam and Boyd, 2003; Boyd and Lam, 2004). Between 2007 and
208 2014 the Tràng An Archaeological Project (Rabett et al., 2009, 2011) conducted a targeted
209 assessment of three prehistoric cave sites within the massif. Most recently, SUNDASIA
210 (2016-2021) has been investigating human adaptation to cycles of sea transgression and
211 regression during the past 60 ka (Rabett et al., 2017a; Utting, 2017; Rabett et al., 2019;
212 Stimpson et al., 2019; O'Donnell et al., 2020) (Figure 2).



ID	Name	Site type	ID	Name	Site type	ID	Name	Site type
1	TAK1	Sediment core	10	TAK10	Sediment core	19	Hang Thung Binh 1	Relict cave
2	TAK2	Sediment core	11	WK-8269	Notch date	20	Động Thiên Hà	Relict cave
3	TAK3	Sediment core	12	WK-8268	Notch date	21	Hang Bói	Relict cave
4	TAK4	Sediment core	13	WK-8267	Notch date	22	Hang Mòi	Relict cave
5	TAK5	Sediment core	14	Hang Công Bình	Relict cave	23	Mái Đá Ốc	Rock shelter
6	TAK6	Sediment core	15	Hang Quàn	Relict cave	24	Mái Đá Vàng	Rock shelter
7	TAK7	Sediment core	16	Hang Vòng	Relict cave	25	Mái Đá Ông Hay	Rock shelter
8	TAK8a	Sediment core	17	Mái Đá Chợ	Relict cave	26	Vụng Chạy	Sediment core
9	TAK9	Sediment core	18	Hang Chùa	Water cave	27	Vụng Thẳm	Sediment core

213

214 *Figure 2: Overview of Tráng An WHS property with sediment cores, radiocarbon dated notch sites and Pleistocene and*
 215 *Early- to Mid-Holocene sites indicated. ¹⁾ after O'Donnell et al. (2020) ²⁾ after Boyd and Lam (2004) ³⁾ after UNESCO*
 216 *(2014a).*

217 The Tráng An massif is part of the North Vietnam orogenic belt and is composed of thinly
 218 bedded to massive Triassic limestone of the **Đông Giao** and **Pa Khôm** formations that have

219 undergone extensive uplift and deformation following the collision of the Indian subcontinent
220 with Eurasia and subsequent activation of the Red River fault (Metcalf, 2017). After
221 denudation, karstification took place under the influence of tropical and sub-tropical climate
222 regimes during which extensive cave systems and deep river valleys formed along faults and
223 fissures in the bedrock. Ongoing erosion caused by high-volume precipitation resulted in the
224 collapse of the cave systems and the formation of a fengcong landscape, comprising enclosed
225 dolines separated by cone and saddle karst formations. Planation was further driven by sea
226 inundations and seasonal flooding that transformed the fengcong into a fenglin topography of
227 karst towers up to 245 m in height and deep intersecting alluvial valleys (Figure 3 a). Today,
228 both these landforms exist side-by-side in Trảng An, illustrating different stages of tropical
229 karst evolution, with fengcong topography dominating in the west (Figure 3 c) and fenglin
230 prevalent in the east. Isolated and heavily eroded karst remnants in the west and northwest
231 frame the central formations and constitute the final stages of a mature karst (Waltham, 2009;
232 Pham et al., 2013) (Figure 3 b).

233 Triassic limestone of the Pa Khôm formation, which underlies the Đổng Giao sequence is
234 exposed in the northwest of the massif where it forms a series of isolated outcrops that rise to
235 a height of 177 m asl. The highest of these outcrops, Núi Dinh, is capped by the Đổng Giao
236 formation (Do et al., 2012). An elevated Quaternary marine terrace, covered by undivided
237 Quaternary sediments, is situated between these formations (Mathers et al., 1996; Tue et al.,
238 2018). This locally unique area rises up to 15 m above the surrounding floodplain and
239 constitutes the only plain that remains unaffected by seasonal flooding (Figure 3 c).



240

241 *Figure 3: Karst landforms of Trảng An. a: karst valley formed in the fenglin or tower karst dominated south and southeast of*
 242 *Trảng An. b: isolated karst towers in the final stage of planation in the southeast of Trảng An. c: 180° panoramic image (left*
 243 *= north, right = south) of the west and northwest extent of the Trảng An massif. A marine terrace stands at 15 m asl and*
 244 *extends along the fengcong dominated western edge with Núi Dinh visible in the distance. The photo was taken after a heavy*
 245 *monsoon rain fall that flooded much of the alluvial plains but left the elevated area that approximates the marine terrace*
 246 *unaffected. [photo credit: TK]*

247 Prior to delta initiation at the end of the LGM (Stanley and Warne, 1994), the Sông Hồng
 248 basin extended towards the southeast into a landmass that occupied the Vịnh Bắc Bộ and
 249 extended past Hainan island (Yao et al., 2009). Rapid sea level rise at the beginning of the
 250 Holocene drowned most of this landmass and by 9 ka BP the sea had transgressed into the
 251 Sông Hồng basin and reached the western fringe of the Trảng An massif. Local sea level
 252 curves for the area place Trảng An at the margin of the maximum extent of the Mid-
 253 Holocene transgression with coastlines extending as far as the western edge of the massif
 254 (Mathers et al., 1996; Mathers and Zalasiewicz, 1999; Lam and Boyd, 2003; Tanabe et al.,
 255 2003a; Tanabe et al., 2003b; Boyd and Lam, 2004; Hori et al., 2004; Tanabe et al., 2006;
 256 Funabiki et al., 2007; Yao et al., 2009; Tue et al., 2018) (see also Appendix A.2). The

257 uncertainty surrounding the exact extent of the transgression, which affected interpretations
258 of palaeoenvironmental reconstructions (O'Donnell et al., 2020) and archaeological findings
259 within Trảng An, prompted the detailed coastline construction presented here.

260 **2. Methodology**

261 *2.1 Field methods and materials*

262 Notch elevations and locations were recorded over three field seasons in September 2017,
263 April 2018 and November 2018 using a Leica GS 15 nRTK (network Real Time Kinematic)
264 GNSS (Global Navigation Satellite System) receiver and Leica TS06 total station
265 accompanied by photographic documentation of each site. The GNSS receiver was connected
266 to the Nam Dinh reference station NTRIP (Networked Transport of RTCM via Internet
267 Protocol) caster. Topography frequently reduced the visible horizon, which resulted in poor
268 Position Dillution of Precision (PDOP) and Geometric Dillution of Precision (GDOP). The
269 distance to the NTRIP caster also resulted in frequently longer-than-ideal lead times to signal
270 fixing. To ensure measurement integrity, control measurements were taken at a local datum
271 point (National Benchmark 140411, U Bò mountain) and an arbitrary fixed point at the
272 project fieldwork base. Multiple, repeated control measurements were also taken at a subset
273 of notch locations. Where a nRTK measurement via NTRIP was not available, measurements
274 were post-processed in Leica Geo Office using Rinex data from a reference station at Nam
275 Định.

276 To enhance measurement accuracy at notch sites, three reference points were recorded for
277 each total station setup near a notch site or centrally within a cluster of notch sites and
278 oriented to the GNSS point locations. In the case of Động Thiên Hà, the notch was inside a
279 cave and the total station was traversed from the GNSS reference points at the boat landing
280 into the cave (Figure 4).



281

282 *Figure 4: Survey of Động Thiên Hà notch site. Left: traversing elevation along the access path into the cave. [photo credit:*

283 *Fiona Coward] Right: surveying the notch inside the cave. [photo credit: TK]*

284 Observations were recorded using a standard reflector where possible and in reflectorless
285 mode when notches were out of reach. Measurements were taken at the roof edge, apex and
286 floor edge of each notch to obtain elevation of tidal maximum, minimum and mean water
287 level following standards established by Pirazzoli (1986) and Trenhaile (2015). With respect
288 to multi-layered compound notches, the intersection between each component was recorded
289 as floor of upper notch and roof of lower notch. In some cases, the notch apex could not be
290 determined. Such sites were subsequently excluded from coastline reconstruction.

291 *2.2 Data processing*

292 Survey results were collated in a single spreadsheet and calibrated to present sea level using a
293 direct measurement at the Hòn Dấu Vietnam Local Vertical Datum set at 0 m national Mean
294 Sea Level (1.41 m EGM96), which enabled our observations to be aligned with previous
295 notch surveys (e. g. Boyd and Lam, 2004; Nguyen et al., 2012a; UNESCO, 2014a). Current
296 tidal range at Hòn Đâu is between 0.4 and 3.7 m (Boyd and Lam, 2004). A minimum tidal
297 range was calculated, based on the difference between elevations of notch floor and roof.

298 Observations were classed into “notch floor”, “apex” and “notch roof” (see also Appendix
299 B.1).

300 Apart from the apex indicating rsl at the time of formation, the elevation difference between
301 the roof of a notch and its floor also indicates tidal range (Pirazzoli, 1986). Notch
302 morphology is influenced by multiple factors that may offset the apex from mean water level.
303 Only three notches had both a clearly defined roof and floor that were neither deteriorated nor
304 modified, which limited data analysis to a single variable of notch apex as the closest
305 indicator for mean sea level.

306 Notch sites across the massif were found to feature different morphological traits, such as the
307 occurrence of more than one notch at different elevations at a single site (compound notch) or
308 variations in the notch profile and depth. Such characteristics are common and may indicate
309 multiple cycles of sea level changes; intermittent still stand in sea level rise/fall; vertical
310 displacement of the notch site; or variation in erosion caused by hydrological, geological,
311 chemical and biological factors. For example, if bioerosion was a driving factor in notch
312 formation, then the eroding species may have caused more erosion within their habitation
313 zone (apex, floor, roof). Other factors, such as chemical, mechanical erosion and salt
314 weathering may have had similar effects (Liew et al., 1993; Boyd and Lam, 2004; Bird et al.,
315 2010; Trenhaile, 2014, 2015, 2016). *In lieu* of radiocarbon dates, we used the elevation of the
316 notch apex and morphological traits to group them into likely phases of stable sea levels. The
317 mean elevation of these groups could then be associated with existing sea level curves
318 (Pirazzoli, 1991; Hori et al., 2004) and dates from previous work in the region (UNESCO,
319 2012, Boyd and Lam, 2004).

320 To determine the optimal number of clusters (N_C), hierarchical clustering (Anderberg, 1973)
321 was performed in R (R Core Team, 2018) using the ‘cluster’ package (Maechler et al., 2019)
322 on a single variable of notch apex elevation. Dunn’s Index (DI) (Dunn, 1974) was used to

323 assess best separation between individual clusters using the ‘clValid’ package (Brock et al.,
324 2008) with a higher DI indicating a better separation. A dendrogram was generated and
325 modified for style in ‘dendextend’ (Galili, 2015). Cluster assignments were exported as CSV
326 and appended to the geospatial notch database in ArcGIS Pro. Descriptive statistics were
327 carried out in SPSS 26 using the ‘means’ function to determine range, min, max, mean, mean
328 error, variance and standard deviation. Proposed clusters were visually assessed for
329 underlying spatial autocorrelation, as these could potentially cause bias in cluster generation
330 and skew rsl predictions. For example, a cluster that contained a small number of sites with a
331 low variance in close proximity to one another was deemed to be spatially correlated and thus
332 aggregated into a single data point. Where individual components within a compound notch
333 were assigned to the same cluster, the survey data were revisited and re-evaluated for
334 ambiguous measurements. Complex compound notches with two individual components may
335 represent the same temporary still-stand with two different tidal amplitudes or a vertical
336 displacement of the geomorphological marker. Long distance measurements that may not
337 have been targeted correctly onto the notch apex, measurements on notches that did not have
338 a clearly developed apex or where a geological feature was erroneously classed as a notch
339 were subsequently excluded from the data set. The process of clustering was then repeated on
340 the resulting final dataset. Once the final clusters were established, the measurements from
341 the individual clusters were summarised and their means were used as the base lines for
342 coastline reconstruction.

343 *2.3 Coastline reconstruction*

344 Mid-Holocene coastlines for Trảng An were reconstructed on the basis of relative sea level
345 change, not detailing isostatic and eustatic contributions, illustrating the extent of the Mid-
346 Holocene sea transgression rather than contemporaneous eustatic sea level. A generalised

347 vertical offset to adjust for isostasy could be applied to calibrate to contemporaneous eustatic
348 sea levels. Most recently, Nguyen and Takewaka (2020) identified variable subsidence and
349 uplift of the Nam Định area of between 1.2 and 1.9 mm/yr in the south and subsidence in the
350 north along a 72 km stretch of the southern half of the RRD coast. Post-Mid-Holocene
351 sediments, predominantly of alluvial origin, were accounted for by averaging depth from
352 published core data from inside and outside the massif (Tanabe et al., 2003a; Tanabe et al.,
353 2003b; Hori et al., 2004; Tanabe et al., 2006; Tran et al., 2013; UNESCO, 2014a; O'Donnell
354 et al., 2020) by adding them as offsets to predicted relative sea levels. Ultimately, we
355 identified three principal areas within the Tràng An massif that were likely to have been
356 differentially affected by alluvial processes and therefore required the application of different
357 offsets (see also Appendix A.4). Palaeo-coastlines for a given sea level were modelled along
358 the contour lines of the SUNDASIA DSM (digital surface model) by automated extraction of
359 contours using adjusted rsl values ($\text{contour} = \text{predicted rsl} + \text{offset}$). Contours were extracted
360 as polygons using the contour function in ArcGIS Pro with the calculated contour value set as
361 the base and an interval greater than the highest peak of the DSM. A smoothing algorithm
362 was applied to each rsl-contour followed by manual adjustments to eliminate irregularities in
363 the topography, such as buildings, roads and trees. A large-scale coastline model for the
364 southeast section of the RRD was derived from a sentinel SRTM DEM by applying the same
365 workflow as for the smaller-scale model.

366 **3. Results**

367 *3.1 Survey results*

368 A total of 172 measurements were taken at 42 individual sites (Table 1, Appendix B.1)
369 distributed within the massif, around its edge and at some isolated outcrops. Ninh Bình city
370 was the only notch site located outside the WHS property. Of these measurements, 72 were

371 of the elevation of the notch apex. Roof and floors were preserved at 21 notches, roofs only at
 372 30 notches and floors only at 2 notches (see Appendix B.2).

Feature type	Mean asl	N	Std. Deviation	Std. Error of Mean	Minimum	Maximum	Range
Notch base	4.5376	70	1.02434	0.12243	2.59	6.30	3.71
Notch apex	3.9132	72	1.04311	0.12293	2.07	5.95	3.88
Notch roof	3.9137	30	0.94144	0.17188	1.93	5.43	3.50
Total	4.1674	172	1.05833	0.08070	1.93	6.30	4.37

373 *Table 1: Summary statistics of all measurements by feature type.*

374 3.2 Cluster analysis

375 Initial clustering on the full data set (N=72) in R returned greatest distance between clusters
 376 at $N_c = 3$ (DI = 0.123), closely followed by a 4-cluster division (DI = 0.107) (Appendix B.3).
 377 Spatial correlation and ambiguous measurements were identified at 39 sites, leaving 33 sites
 378 for the final clustering.

379 Final clustering at $N = 33$ (Figure 5) also produced the greatest distance between clusters at
 380 $N_c = 3$ (DI = 0.235) resulting in three distinct notch sequences with mean elevations of 3.2 m
 381 (N = 22, SD = 0.430), 4.6 m (N = 7, SD = 0.243) and 5.6 m (N = 4, SD = 0.092) (Table 2).

382 Clustering of 22 notches into the lower sequence, however, resulted in the inclusion of
 383 multiple components of compound notches into the same cluster. This conflict was partially
 384 resolved by increasing the number of clusters to $N_c = 4$ (DI = 1.446) (Table 3).

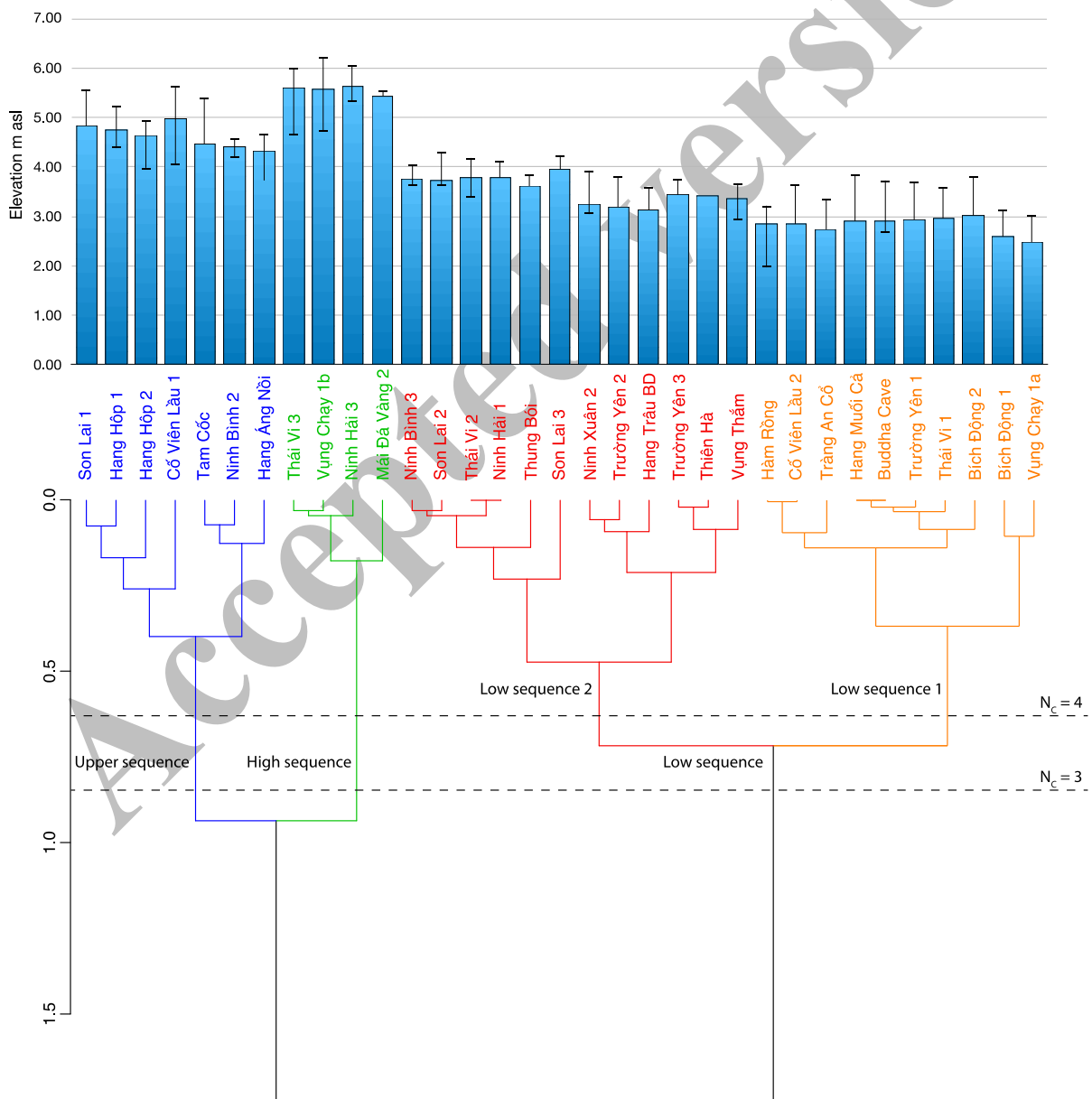
Sequence Level	Lower			Upper			High		
	Floor	Apex	Roof	Floor	Apex	Roof	Floor	Apex	Roof
N	7	22	21	5	7	7	3	4	4
Mean	3.1	3.2	3.8	4.1	4.6	5.2	4.9	5.6	6.0
Std dev.	0.583	0.430	0.349	0.237	0.243	0.422	0.379	0.092	0.284
Std. Error	0.220	0.092	0.076	0.106	0.092	0.160	0.219	0.046	0.142
Min	1.99	2.49	3.03	3.74	4.33	4.60	4.64	5.44	5.57
Max	3.63	3.98	4.31	4.38	5.01	5.64	5.34	5.65	6.23

385 *Table 2: Summary of averaged notch metrics after classification into three clusters.*

Sequence Level	Lower 1			Lower 2		
	Floor	Apex	Roof	Floor	Apex	Roof
N	2	10	10	5	12	11
Mean	2.3	2.8	3.5	3.3	3.6	4.0
Std dev.	0.499	0.173	0.300	0.310	0.271	0.237
Std. Error	0.353	0.055	0.095	0.139	0.078	0.071
Min	1.99	2.49	3.03	2.96	3.15	3.60
Max	2.70	3.03	3.85	3.63	3.98	4.31

386 Table 3: Summary of averaged notch metrics after subdivision of lower notch sequence.

387

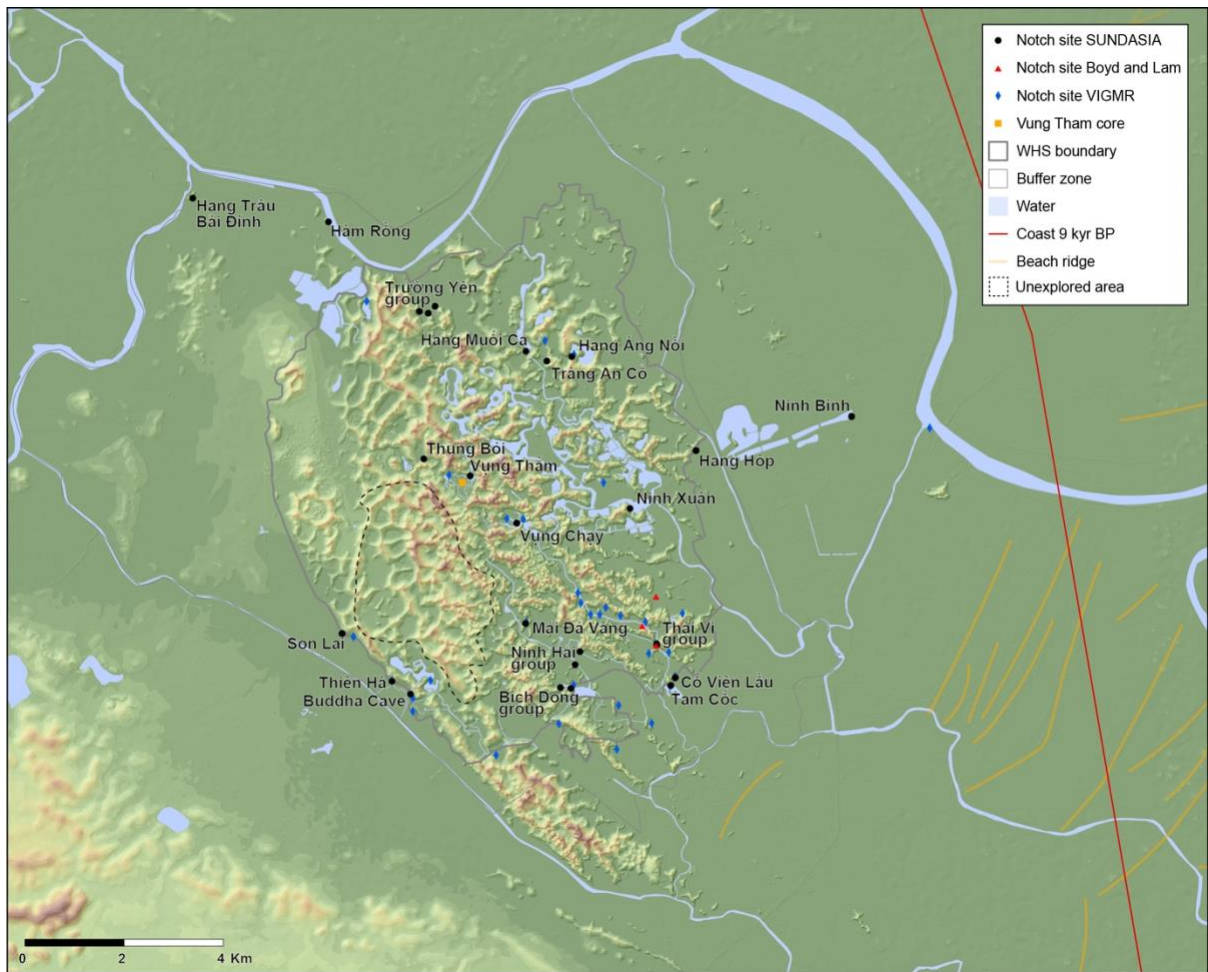


388

389 *Figure 5: Final dendrogram of aggregated measurements on notch apex (N = 33). Optimal clustering was achieved at $N_c =$*
390 *3. At $N_c = 4$ a possible subdivision of the low sequence partially resolves grouping individual components of compound*
391 *notches into the same cluster. The bar diagram shows the elevation of notch apices whilst whiskers indicate elevations of*
392 *notch floor and roof (where present).*

393 *3.3 Notch distribution*

394 Notches were found to be most frequently distributed along karst towers and cones on the
395 eastern and southern extent of the Trảng An massif and its eastern open karst valleys, where
396 they continuously extended in excess of 100 m along the vertical cliffs. Some central open
397 and enclosed dolines also featured notches, such as Vụng Thám, Thung Bói and Vụng Chạy.
398 Notches also occurred, albeit less frequently, in the west and north of the massif where they
399 were observed on limestone boulders or as short sections on isolated karst remnants. Notches
400 were found to be absent on the north-western Pleistocene marine terrace. An area within the
401 western and central part of the property including a group of enclosed dolines with a potential
402 for further notches remains unexplored due to limited accessibility and time-constraints
403 (Figure 6). The higher density of notch sites in the east of the massif is likely due to its
404 orientation towards the coast. Beach ridges as near as 1 km from the edge of the massif are
405 detectable in elevation maps and illustrate that the eastern part was exposed to wave action.
406 Here, planation is more advanced than in the west, which may also be attributable to its
407 exposure to wave action during inundation. Inundations would have also advanced
408 westwards, leaving the east submerged for longer than the west. All these factors would have
409 favoured the formation of notches in the east over the sheltered west, where hills and ridges
410 also have lower gradients and dolines are more frequently closed and have more elevated
411 floors than in the east, limiting or prohibiting flooding.



412

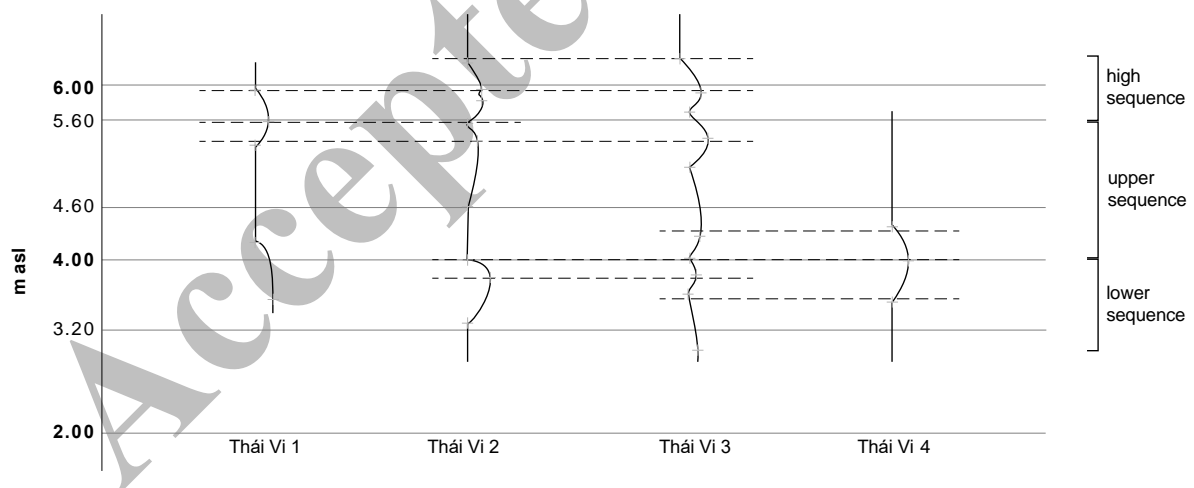
413 *Figure 6: Distribution of surveyed notch sites today in relation to Vung Thám core at the center of Tràng An (O'Donnell et*
 414 *al. 2020). Notches are more abundant, more developed and found at higher elevations in the palaeoshore-facing southeast*
 415 *of the massif. Notch sites VIGMR after (Nguyen et al., 2012a; Pham et al., 2013; UNESCO, 2014b). Coast 9 ka BP after*
 416 *Tanabe et al. (2003b).*

417 Two notches were recorded at Ninh Nhật and Ninh Xuân with respective elevations of 32.83
 418 m and 32.44 m asl. These notches only survive as faint marks in tall vertical cliffs. Such
 419 notches likely pertain to earlier Quaternary transgressions and illustrate the amount of uplift
 420 the area has undergone since their formation.

421 3.4 Notch morphology

422 The notches of Tràng An are morphologically varied with morphotypes encompassing simple
 423 single element types as well as complex multiple element compound notches. Some feature

424 irregular corrosion patterns whereas others show polycyclic corrosion patterns in the form of
 425 completely separated or superimposed compound notches. Erosion along vertical fissures and
 426 between bedding planes at some sites obscured notch features, which made identification and
 427 classification challenging. This was particularly evident at Thái Vi 2/3 (Figure 7). These two
 428 complex compound notches comprise closely spaced, partially overlaying bands with
 429 disturbance from eroded horizontal bedding planes, widened fissures and partial cliff
 430 collapse. Their upper and middle sequences consist of two individual and slightly
 431 overlapping components both in the upper sequence at 5.9 m, 5.4 m and 4 m, and in the lower
 432 sequence at 3.6 m. Thái Vi 1 and 4 are of a simpler morphology with Thái Vi 1 consisting of
 433 two discernible erosional sequences that were recorded at the same elevation as the lower
 434 component of the upper and the upper component of the lower sequences of Thái Vi 2. Thái
 435 Vi 4 consists of only one sequence at the same elevation as the upper component of the lower
 436 sequence of Thái Vi 2.



437

438 *Figure 7: Schematic profiles of Thái Vi 1 – 4, their elevations and attribution to the identified three stable sea level*
 439 *sequences.*

440 Continuous erosion has reduced notch depth and height particularly in the upper and high
 441 sequences, which had a direct impact on tidal range estimations. Collapse of undercut cliff
 442 sections also led to fragmentation of notches or partially missing notch roofs. This type of

443 mechanical erosion is observable at Vụng Chạy, Thái Vi, Tràng An Cỗ, Son Lai and Hang
444 Hốp. Freshly exposed limestone is visible as bright and frequently orange- to brown-coloured
445 sections in the otherwise grey to dark grey patinated limestone cliffs. The collapse sites
446 observed in Tràng An were all patinated and lacked basal collapse piles, indicating that the
447 cliff sections broke away some time ago. In contrast, examples of fresh collapses were
448 observed in Cát Bà/ Hạ Long Bay with collapse piles at their bases (Figure 8). At Hang Áng
449 Nồi and Mái Đá Vàng similar processes are likely responsible for the survival of only short
450 and shallow sequences of formerly more substantive notches.



451

452 *Figure 8: left: Collapse at Thái Vi notch by ongoing planation through undercutting of the cliff by notches. The collapse*
453 *most likely occurred during the Mid-Holocene highstand as some superficial erosion marks are visible within the collapse*
454 *scar in-line with the uppermost notch sequence. Right: Recent collapse of section of limestone cliff at Cát Bà by the same*
455 *process. [photo credit: TK]*

456 Post-formation vertical erosion was more prevalent in the upper and high notch sequences
457 than in the lower, being well advanced at Cỗ Viên Lầu, Tam Cốc and Vụng Chạy but less
458 pronounced at Bích Động and Thái Vi (Figure 9). Much of the notch surfaces were heavily
459 obscured, but the upper edges were visible as a horizontal line that was more noticeable
460 where it crossed non-horizontal bedding planes.



461

462

463

Figure 9: Notch types observed at Tràng An (top left to bottom right): deep notch at Tam Cốc, single single U-shaped notch at Vụng Thảm, shallow notch at Ninh Hải (3), V-shaped notch at Trường Yên 2, bioerosion scars on single U-shaped notch

464 *at Tràng An Cổ, V-shaped notch formed in foot cave at Hàng Muối Ca, polycyclical notch with two distinct phases at Hang*
465 *Hộp, multi-sequence polycyclical notch at Thái Vi 2 (left) and 3 (right). [photo credit: TK]*

466 A notch with a bench of 1 – 2 m depth had formed in the base of a sloping limestone ridge at
467 Son Lai (Figure 10). The site is located in a protruding outcrop along the western margin of
468 the massif, just south of the elevated Pleistocene terrace. The lateral offset between notch
469 floor and roof roughly coincides with the slope of the limestone outcrop. The base of the
470 bench, however, is vertical and does not follow the slope above. The notch has a height of 1.5
471 m with an irregular profile caused by large scallop-like pits, which measure c. 20 – 30 cm in
472 length. The morphology of the Son Lai notch is unique within Tràng An and its features may
473 be attributable to its location. A narrow eastward-oriented channel that separated Tràng An
474 from the surrounding main land during the Mid Holocene likely drained some of the tidal
475 flats west of massif. During low tide, the increase in water volume passing through the
476 channel would have caused an increase in water flow as well as some turbulences where the
477 water flow was redirected from an easterly to a southerly direction where the outgoing tide
478 met the limestone massif at the level of Son Lai.



479

480 *Figure 10: A notch formed in a limestone hill at Son Lai. The sloping rockface has left the notch roof recessed from the*
481 *protruding notch floor, following the gradient of the hill. Irregular pits or scallops line the back of the notch [Photo credit:*
482 *TKJ]*

483 *3.5 Lower notch sequence*

484 Notch profiles were found to be either V-shaped or U-shaped with an almost horizontal roof
485 and, where exposed, an outwards sloping floor. Notches at 2 – 3 m asl were frequently filled
486 with alluvium to just above the notch floor. Being subject to flooding during the monsoon
487 season, their lateral development is likely to be ongoing. Notches at 3 – 4 m asl were found to
488 be frequently equipped with concrete or mottled floors and used as storage, habitation, or
489 places of worship, which prevented us from obtaining a floor elevation measurement.
490 Notches that horizontally extend more than 2 m into the bedrock are uncommon but were
491 recorded at Tam Cốc, Ninh Bình, Buddha Cave, Ninh Xuân and Hang Muối Cả. The latter is
492 the most extensive notch in our data set. Classed as a cave, it extends over 59 m into Cái Hạ
493 Mountain at an elevation of 2.9 m asl with a maximum height of 4.8 m, measured from an
494 artificial floor that covers the entire space. The surface of this feature is entirely covered with
495 small, c. 5 cm long, scallop-shaped erosional pits. Scalloping occurs on notches in the
496 supratidal zone and can be caused by grazing limpets (Kazmer and Taborosi, 2012; Kazmer
497 et al., 2015), but a purely solutional origin, however, may also be possible. Scalloping was
498 frequently observed in notches belonging to the lower sequence.

499 Vertical ridges that frame the enclosed doline of Vụng Thảm feature a series of well-
500 developed basal notches that are partially below the current ground surface. Their almost
501 horizontal roof could measure up to 1.5 m in depth with a slightly outward declining floor.
502 Notches in the lower sequence frequently occur as fragments on peripheral outcrops and
503 isolated boulders inside enclosed and open dolines. In Thung Bói, numerous boulders with
504 notches at 3.6 m asl were found distributed across the doline floor (Figure 11). Similar

505 observations of erosional features on isolated boulders were made in Lau valley, just north of
506 the Son Lai notch. These erosional features are not well-developed and may not be *in situ* but
507 they serve as indicators for the presence of water over a prolonged period of time. A poorly
508 defined notch at c. 3.4 m is located near Hang Trâu Bái Đính in an isolated karst outcrop
509 (Figure 12). Its base was entirely embedded in sediments but its roof suggests a v-shaped
510 profile with scalloping occurring on the exposed surface. It is the most north-western notch of
511 our survey and provides a minimum extent of marine transgression for the northern part of
512 the massif.



513

514 *Figure 11: One of numerous notch-incised boulders strewn across the doline floor of Thung Bói.*



515

516 *Figure 12: A poorly defined notch in a small limestone outcrop near Hang Trâu Bái Bình in the northwest of the property.*

517 *3.6 Upper notch sequence*

518 Notches that fall within the 4 – 6 m bracket were found to be laterally less developed
519 compared to the lower notch sequence and reached a depth of less than 1 m. Their mean
520 height does not differ significantly from the lower sequence but shows greater morphological
521 variation.

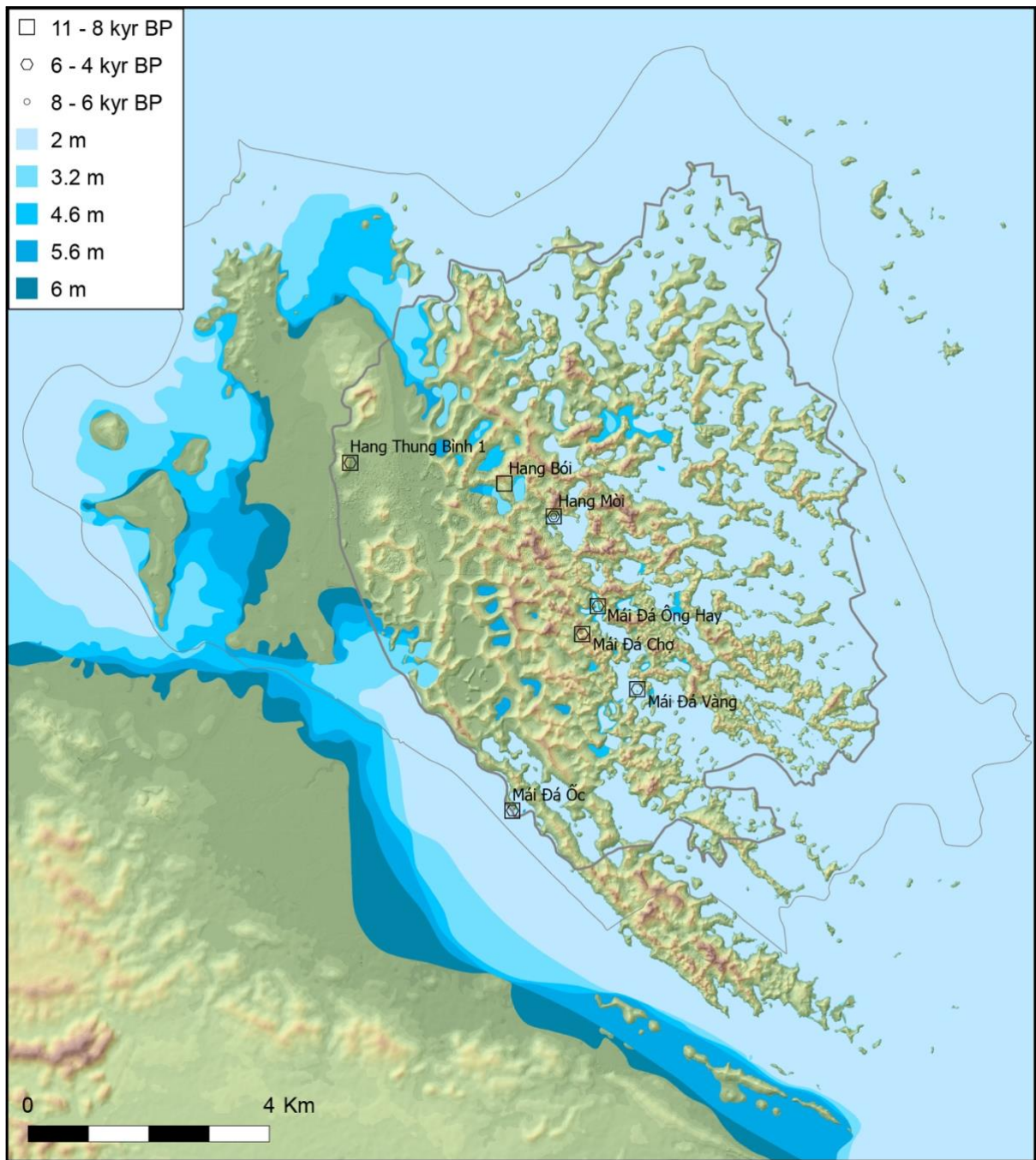
522 Notches at the highest elevations of 5 – 6 m are frequently compound notches and of shallow
523 depth. Those that line the northern cliffs of the broad and open lower Bích Động valley are
524 U-shaped with a single component which is less than 0.5 m high and equally deep. They
525 incise the cliffs at a mean elevation of 5.6 m asl. Further upstream and near the
526 archaeological site of Mái Đá Vàng, a faint secondary notch at 5 m asl was visible below a
527 shallow notch at 5.4 m asl.

528 Notches at Thái Vi show the highest complexity among the surveyed notches, with up to four
529 individual overlapping notches discernible over the full height of the compound notch of 4.6
530 – 6.3 m asl. These cut laterally up to 1 m into the south-facing cliff of Núi Voi Phục
531 mountain and the cliffs along the adjacent valley and can be followed for several hundred
532 meters.

533 While the separation of the individual components into a lower and upper sequence is also
534 observable in other notches in the immediate area, the complexity of the upper components
535 will require dating evidence to establish the chronological relationship between them which
536 can offer a clue into their development.

537 *3.7 Coastlines*

538 Based on our dendrogram outputs, we reconstructed five different surfaces that model the
539 coastlines derived for the lower (3.2 m), upper (4.6 m) and high (5.6 m) sequences.
540 Additional surfaces were constructed at 2 m and 6 m to illustrate observed tidal maximum at
541 Vụng Chạy 1b (6.2 m) and minimum at Hàm Rồng (2 m). Relative mean sea level values
542 varied by 0.67 m for the upper sequence and 1.49 m for the lower sequence (Figure 13).
543 Direct observations of tidal ranges where floors and roofs were exposed and/or preserved
544 well enough for measurements were made at 15 sites. The tidal range for the lower sequence
545 was 20% less than that of the combined upper and high sequences. The difference in tidal
546 range between the upper and high sequences was negligible (Table 4).



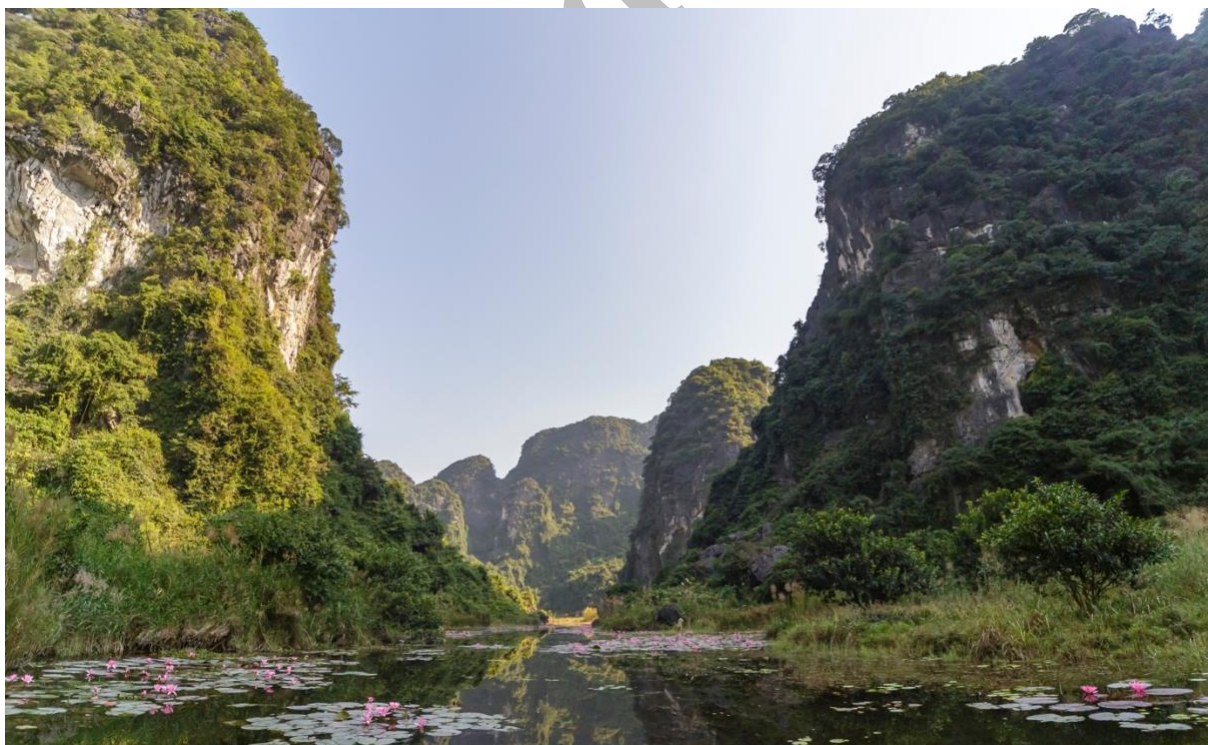
547

548 *Figure 13: Coastline model during Middle-Holocene transgression in context with radio carbon dated archaeological sites*
 549 *that fall between 11 ka and 4 ka BP.*

Sequence	Lower	Upper	High
N	7	5	3
Mean Tidal Range	0.8	1.0	1.2
Std. Dev.	0.257	0.421	0.405
Std. Error	0.097	0.188	0.234
Variance	0.066	0.177	0.164

550 *Table 4: Tidal range estimation for notch sequences.*

551 Based on our model, landscape inundation progressed from east to west across Tràng An and
552 rapidly progressed into the east of the massif with its valleys, poljes and open dolines, such as
553 the Bích Động and Thái Vi valleys, most of which comprise near-vertical cliffs (Figure 14).
554 After initial flooding, the shoreline within this part of the massif remained relatively stable
555 throughout the Mid-Holocene transgression. Lateral shoreline progression in the northwest of
556 Tràng An was more dynamic due to the Pleistocene terrace and its low graduated slopes.
557 Standing at 10-15 m asl, the terrace extends southwards along the western extent of the karst
558 and into the polje east of Thung Chùa. Here, the shoreline gradually advanced with rising sea
559 level. The topography between the Tràng An massif and the western uplands is lowest along
560 the Sông Mới channel which became flooded as the sea level exceeded 4.6 m rsl, separating
561 Tràng An from the main land. As the sea level reached its maximum, the channel reached a
562 width of up to 1 km.



563

564 *Figure 14: Landloss in valleys with steep cliff faces was marginal and did not significantly alter the coastline as sea levels*
565 *rose.*

566 Enclosed dolines in the west and central massif with floor levels near or below 5 m became
567 increasingly affected by rising sea levels. The internal environment changed from dry to
568 brackish swamp, saltmarsh, tidal and finally fully flooded hong (marine lake). A general
569 trend was observed wherein enclosed central dolines were flooded from the northeast and
570 southeast, with those adjacent to the Pleistocene terrace found to be above the highest
571 predicted sea level of 6 m. Notches with apex levels of around 3.5 m were recorded at Vụng
572 Thấm and Thung Bói, indicating permanent flooding under a tidal regime during the Mid-
573 Holocene.

574 Compound notches were more common along the cliffs of open karst valleys and poljes in
575 the south and southeast, indicating that this area was affected most and the longest by
576 inundations. Here, relative sea levels reached a maximum of at least 5.6 m but could have
577 potentially reached 6 m asl. The high sequence has, however, not been securely dated yet
578 thus leaving the possibility of an earlier Pleistocene date for some of the notches. The
579 complex morphology of the lower two sequences indicates that either transgression or
580 regression was not linear but underwent phases of stagnation allowing for the formation of
581 compound notches with two distinct apexes within one larger notch. These notches have been
582 previously dated from cemented oyster shells (Boyd and Lam, 2004; UNESCO, 2014).

583 **4. Discussion**

584 *4.1 Dating marine inundation at Tràng An*

585 The presence of at least three, possibly four sequences of notches suggests that Tràng An has
586 experienced multiple phases of prolonged and relative stable sea levels of +3.2 m, +4.6 m and
587 +5.6 m. As there are no new dates from the notches at this stage, a chronology had to be
588 estimated by association with previous work. Boyd and Lam (2004) radiocarbon dated oyster
589 shells from notches in the Tam Cốc area at 5.4 m asl to 5740 – 5500 cal BP (Wk-8267) and at

590 4 m asl to 5550 – 5270 cal BP (Wk-8268) BP, which coincide with the upper and high notch
 591 sequences from our model. While those authors do not state the exact location of the dated
 592 notch, the given name likely pertains to the Tam Cốc / Bích Động area, which was also
 593 included in the present survey. Similar dates were established during a geomorphological
 594 survey for the UNESCO WHS dossier (table 5) (UNESCO, 2014). The elevations stated in
 595 the dossier were taken from the base of the notch and do not coincide with the elevations of
 596 our surveys. The associations with individual samples from within compound notches,
 597 particularly Thai Vi, therefore carry some uncertainty. On the basis of the available dating
 598 evidence, the upper sequence of our model is cautiously attributed to the peak of the Mid-
 599 Holocene transgression, while the lower sequence likely pertains to the later Holocene. An
 600 extensive sampling and dating campaign of palaeo-sediments from notch sites is needed to
 601 provide a clearer picture of the time frames involved. The presence of the lower sequence at
 602 most of the surveyed sites indicates that much of the plains in and around Tràng An were
 603 almost certainly fully submerged for an extended period of time during the Mid- to later
 604 Holocene.

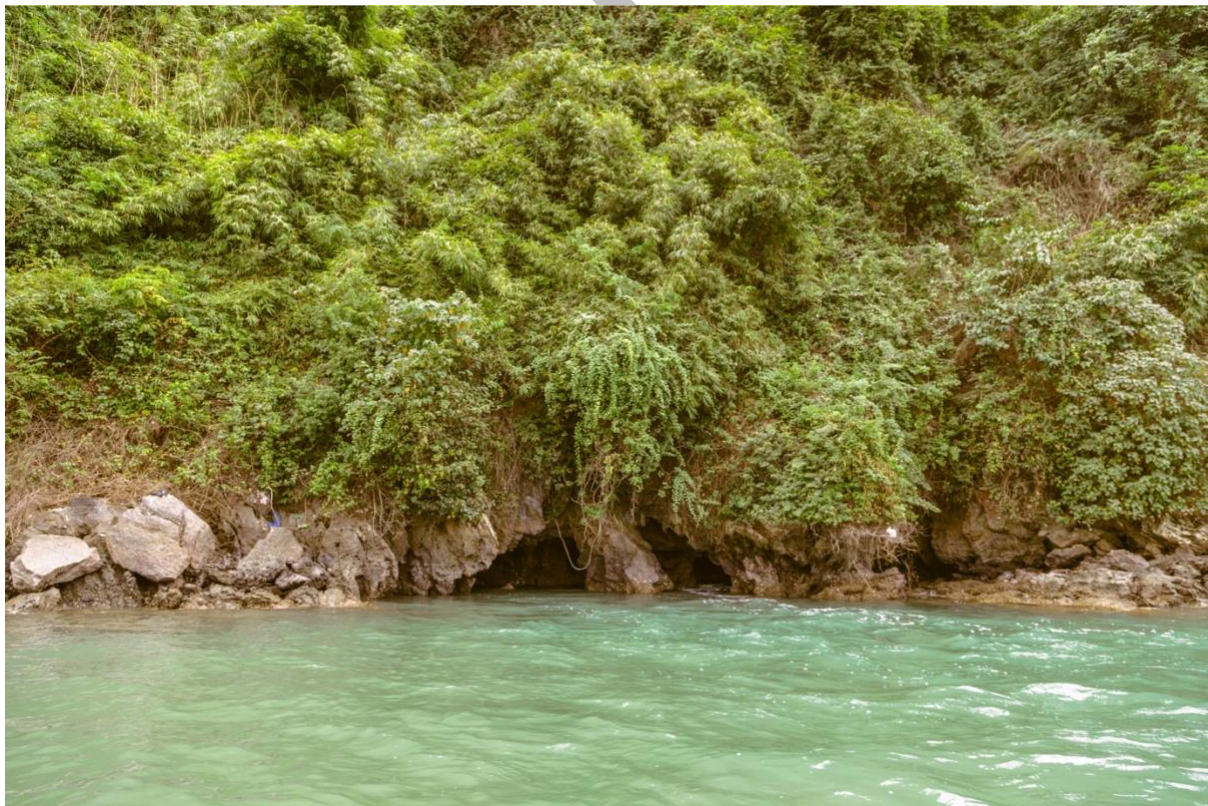
Site	Sample location	ASL	¹⁴ C Age	Cal. BP
Thái Vi 2	Notch base	3.3	4390 ± 310	4530 ± 320
Tam Cốc	Notch base	2.2	4220 ± 290	4350 ± 300
Đồng Thiên Hà	Notch base	2.3	5230 ± 310	5390 ± 320
Đồng Thiên Hà	Notch base	2.3	5430 ± 315	5500 ± 325
Đồng Thiên Hà	Notch base	2.3	5110 ± 230	5260 ± 240

605 *Table 5: Radiocarbon dates from Oyster samples taken during a geomorphological survey for the UNESCO WHS dossier*
 606 *(UNESCO, 2014). Elevations were re-taken for this study.*

607 4.2 Within-sequence variation of notch elevations

608 The variation of sea level values within the upper sequences of 0.67 m, or 1.23 m including
 609 the upper Tam Cốc / Bích Động notch sequence, and 1.49 m for the lower sequence adds
 610 some ambiguity to our coastline reconstructions.

611 Within-sequence variation in notch elevations may be caused by hydro-geomorphological
612 factors such as restrictions to water flow, which may have influenced water-levels in some
613 enclosed flooded dolines (hongs). Water flow in these hongs was likely controlled by foot
614 caves, subaerial caves and other small conduits. While some foot caves were large enough to
615 provide sufficient flow during a tidal cycle, some hongs may have experiencing a reservoir
616 effect where retention times were larger than the tidal period. Experiencing permanently
617 raised water levels would have influenced notch formation, with an elevated notch apex and
618 potentially decreased notch height. High-volume precipitation during monsoons would have
619 added to the water volume in a hong, amplifying the tidal reservoir effect and potentially
620 further altering notch morphology. Such reservoir effect in a hong was observed at Cát Bà
621 Island/ Hà Long Bay, Vietnam and corroborated by local informants (Leonard 2020, pers.
622 comm.) (Figure 15) and is known to take place in choked coastal lagoons (Kjerfve, 1994).



623

624 *Figure 15: Small cave draining a series of interconnected tidal on Cát Bà Island. The restricted flow rate causes a*
625 *permanent elevated water level inside the dolines.*

626 Changes in pH, salinity and temperature would have also impacted the biodiversity in a hong.
627 The effects of these factors were documented in Cát Bà/ Hạ Long Bay by Cerrano et al.
628 (2006) and may be detectable in corresponding sediment core profiles. A core obtained by the
629 SUNDASIA project within the enclosed Vụng Thảm doline, near to the Hang Mòi
630 archaeological site, did not contain a Mid-Holocene sequence (O'Donnell et al., 2020);
631 however a second core obtained by the project from the Vụng Chay open doline is under
632 analysis and may contain a more complete stratigraphy.

633 Several possible interpretations of our notch data must be considered. Whilst our model
634 focuses on the Mid- to Late Holocene transgressions as the main cause for notch formation,
635 earlier Pleistocene sea transgressions are likely to have formed marine notches in this massif.
636 Late-Pleistocene transgressions that occurred between 120 – 30 ka BP with rsl at or below
637 Mid-Holocene levels in conjunction with subsequent uplift (Lambeck, 1990; Lambeck and
638 Chappell, 2001) could have left notches at similar elevations that were then re-occupied
639 during the Mid-Holocene transgression. MIS-5 notches at 4 – 6 m asl were recorded in the
640 Mekong delta and Palawan (Lap et al., 2000; Omura et al., 2004) and notches at this level in
641 the southeast of Trảng An may have formed during that period. Resolving the complex
642 processes observed in the Trảng An notches requires the establishment of a comprehensive
643 chronology for the Trảng An notches.

644 *4.3 Implications for archaeology*

645 Several historic communities, most notably the 10th century Hoa Lư ancient capital and, more
646 recently, the provincial capital have been established on the edge of the massif.

647 Archaeological evidence from Trảng An indicates human presence within the massif that
648 extends back to at least 30 ka BP (Rabett et al., 2009; Rabett et al., 2011; Nguyen, 2012;
649 Nishimura and Phan, 2012; Reinecke, 2016; Rabett et al., 2017b). While the vegetation

650 within the upland karst remained mostly stable throughout that time (Rabett et al., 2017b),
651 relative sea level rise from the Early-Holocene through to the Mid-Holocene inundated much
652 of the surrounding plains (Tanabe et al., 2003b) introducing marine taxa, notably mangrove
653 plants, marine-molluscs and crabs to the massif (O'Donnell et al., 2020).

654 The absence of Pleistocene archaeological sites within the plains of the RRD is likely due to
655 Holocene delta progradation and sea transgression, which led to a loss of much of the
656 Pleistocene landmass that extended hundreds of kilometres east of the modern Vietnamese
657 coastline while the remaining delta has been intensively reshaped by fluvial processes.

658 Excavated evidence suggests that Pleistocene hunter-gatherers in this region tended to favour
659 a terrestrial-based diet (Oxenham et al., 2018; Jones et al., 2019) and the archaeological
660 evidence from Trảng An is largely consistent with this (Rabett et al., 2009; Stimpson et al.,
661 2019). The recovery of perforated neritid shells from three archaeological cave sites in the
662 massif implies, however, that while there is negligible evidence for marine resource use on-
663 site prior to the Mid-Holocene, long-standing links appear nonetheless to have existed with
664 the coast, extending back to as early as c. 17 ka cal BP (Rabett et al., 2019). Changes in the
665 range of lithic raw materials utilised through time, from greater diversity before the LGM to
666 reduced diversity thereafter (Phan, 2014; Utting, 2017), also hints that greater mobility may
667 have been a feature of late Pleistocene communities; a contention that finds further support
668 from preliminary lithic provenancing work and geological survey (Nguyen et al., 2012b). As
669 such, the hunter-gatherer groups that frequented Trảng An may also have incorporated sites
670 along the palaeo-coast in their annual or super-annual movements.

671 The Mid-Holocene sea transgression coincided with the establishment of local ceramic
672 technocomplexes, most notably the Đa Bút, which is believed to have emerged as an
673 adaptation to the transformation of the RRD basin from an inland to a coastal environment
674 (Oxenham et al., 2018). While the Đa Bút is commonly attributed to open air sites (Nguyen,

675 2005), excavations in Tràng An, particularly at the site of Hang Mòi, demonstrate that caves
676 continued to form an important part of funerary activities (Rabett et al., 2017a). The
677 zooarchaeological data recovered from Hang Mòi relate to a shift in subsistence strategy to
678 include marine resources in addition to staples from the forest interior and upland habitats
679 (O'Donnell et al. 2020).

680 Our model suggests that Tràng An was separated from its surrounding uplands in the west
681 and north by 300 m to 700 m of water during the Mid-Holocene high stand, between 6 ka and
682 5 ka BP. Notches at Hang Trâu Bái Đính and Son Lai show that the sea transgressed past
683 previously proposed shorelines, which have suggested that only the east of Tràng An was
684 affected by inundation (Tanabe et al., 2003b). Inhabitants of the Tràng An massif would have
685 been isolated from or had only limited access to the mainland for the most part of the 6th
686 millennium BP. Locations for habitation would have been dictated by the advancing sea,
687 cutting off much of the isolated peaks and ridges in the east and northeast and submerged
688 previously occupied sites like Mái Đá Ông Hay and Mái Đá Ốc (Figure 16).



689

690 *Figure 16: The limestone outcrop that accommodates Mái Đá Ốc (indicated) is almost entirely surrounded by flood plains.*

691 *The rockshelter would have been either entirely surrounded or, more likely, submerged during the Mid-Holocene highstand.*

692 Sites located either within or with land-access to the north-western marine terrace during the

693 Mid-Holocene high stand, such as Hang Mòi, Hang Bói, Hang Thung Bình 1, Mái Đá Ốc,

694 Mái Đá Chợ, Mái Đá Ông Hay and possibly Hang Trống, were occupied during the

695 Pleistocene/Holocene transition but with an unclear chronology for the Mid-Holocene. A

696 general absence of ^{14}C dates between 8 ka and 6 ka BP from the available archaeological

697 record (with the exception of two dates from Hang Mòi from around 7 ka BP) may be related

698 to a shift in site location choice in the light of the changing environment but could also be

699 related to heightened monsoon precipitation that may have caused erosion of archaeological

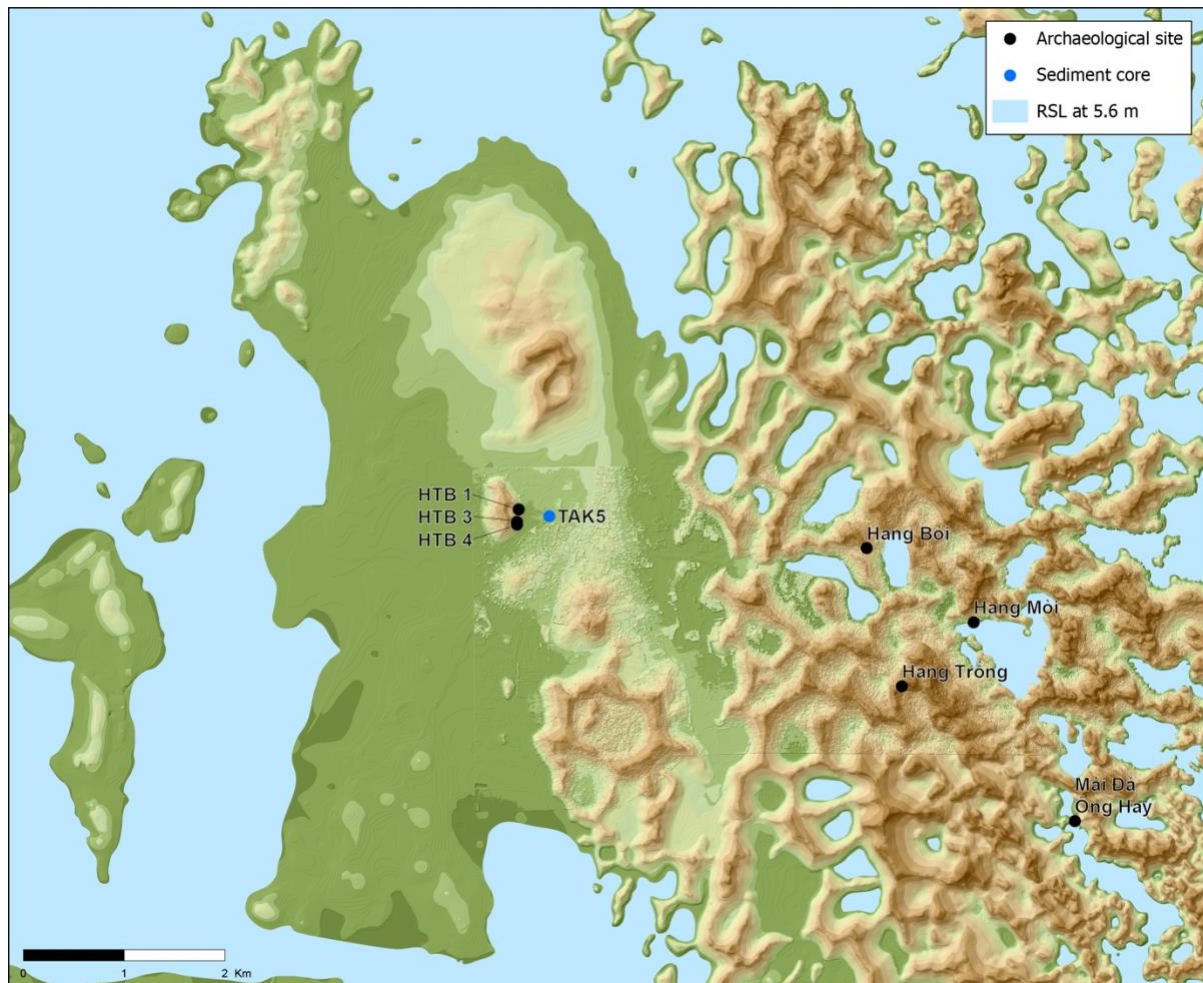
700 strata. Remnants of sediments can be found adhered to the cave wall more than 1 m above the

701 current floor level in Hang Thung Bình 1, Hang Mòi and Hang Bói, with the latter suggesting

702 recurring activity that reaches back as far as the Upper Pleistocene but can also be observed

703 today (Rabett et al., 2011). Such features and observations demonstrate that some relict caves
704 still experience phases of hydrological activity with significant erosion of sediments.

705 At Hang Thung Binh 1, some form of hydrological activity of this otherwise inactive cave
706 was evident in a phase of disturbed sediments overlying late Pleistocene deposits, in turn
707 overlaid by Neolithic (Mán-Bạc) strata. This context comprised of a layer of sediments mixed
708 with Đa Bút pottery sherds that were exposed to flowing water, giving them a distinct ‘water-
709 rolled’ appearance. The paucity of Mid-Holocene evidence is most likely a result of increased
710 precipitation and a wetter environment eroding sediments from the cave rather than a
711 decrease of human activity during that time. Thung Binh Hill is located at the centre of the
712 Pleistocene terrace and its caves overlook the plains that lie between the hill and the edge of
713 the limestone massif, affording superior views across the only remaining plain in a Mid-
714 Holocene marine archipelago, making it an ideal habitation site (Figure 17). Faunal remains
715 from lower occupation layers contain several species of deer (Cervidae), which inhabited the
716 plains that surrounded Thung Binh Hill and likely persisted into the Holocene. Along with
717 access to terrestrial resources, the coast would have been within walking distance in most
718 directions, giving access to marine resources. Palynological assessment of the TAK5
719 sediment core that was taken at the foot of Thung Binh Hill revealed the presence of true
720 mangrove taxa (*Rhizophora* spp., *Sonneratia* spp.) along with backmangrove associated types
721 make up 2.5 – 15% of the pollen, suggesting a weak marine influence on the area. Grasses
722 dominate the assemblage (85%) with ferns as well as coniferous and temperate trees also
723 evident. Given that the marine terrace stood more than 10 m above the Mid-Holocene high-
724 tide level it is likely that mangrove pollen in this elevated area originate from the near-by
725 shore.

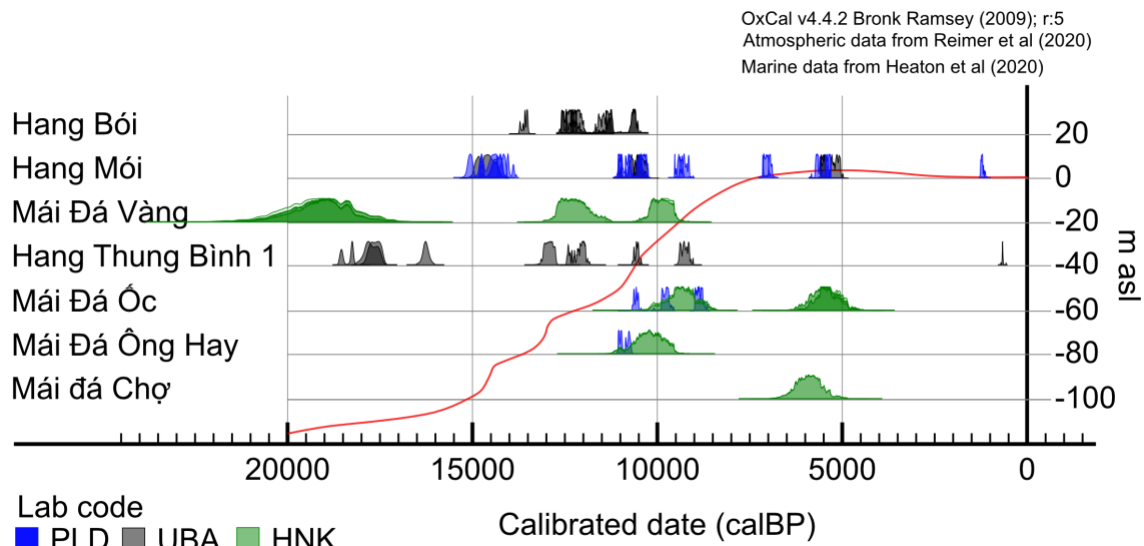


726

727 *Figure 17: Pleistocene terrace at proposed Mid-Holocene highstand, with relevant caves and TAK5 sediment core marked.*
 728 *(Abbreviation HTB = Hang Thung Bình).*

729 Higher elevation sites such as Hang Bói (Rabett et al., 2009) and Hang Trông (Rabett et al.,
 730 2017) appear to have been abandoned as the coastline encroached onto the massif, perhaps
 731 coinciding with a shift in subsistence strategy away from terrestrial to marine resources. Low
 732 elevation rock shelters such as Mái Đá Ốc and Mái Đá Ông Hay that were occupied prior to
 733 the transgression were abandoned as they became affected by rising sea levels (Figure 18).
 734 Elevated cave sites and rock shelters such as Hang Mòi, Mái Đá Vàng and Mái Đá Chợ
 735 continued to be occupied throughout the transgression cycle, with the introduction of a
 736 marine component to forager diet, reflected in an increase of marine taxa in the
 737 archaeological record (Nguyen, 2012; Nguyen and Nguyen, 2012). Hang Mòi, located in an
 738 enclosed doline in the centre of the massif that was flooded during the high stand, produced

739 evidence for occupation spanning from the late Pleistocene through to the late Holocene. The
 740 cultural assemblage from the Mid-Holocene layers was dominated by Đa Bút ceramics with
 741 an under-representation of lithics, whilst faunal remains indicate a mix of inland terrestrial
 742 and marine-based subsistence (Rabett et al., 2019; O'Donnell et al., 2020).



743
 744 *Figure 18: Clustered view of radiocarbon dates from excavated archaeological sites with Holocene dates in Trảng An and*
 745 *calibrated sea level curve for the RRd delta (after Tanabe et al., 2006).*

746 With the possibility of a temporary isolation of Trảng An from the mainland, procuring non-
 747 local raw materials, such as lithics for stone tool production would have posed a challenge.
 748 Evidence that raw materials were imported or exchanged over long distances comes from
 749 lithic assemblages from Trảng An. Whilst primarily composed of unretouched expedient
 750 limestone tools (60 – 95%), these contain a significant minor proportion of tools made of
 751 igneous raw material. The ratio of igneous tools to limestone tools can vary greatly, even
 752 between sites in the same karst tower. At Hang Thung Bình 1 igneous tools account for
 753 14.6% of the assemblage (N = 260), compared to 39.2% at Hang Thung Bình 3 (N = 265).
 754 This difference suggests significant variability in occupation or use between sites that are less
 755 than 100 meters from each other. Overall raw material composition at other sites throughout
 756 the complex varies but changes in assemblage raw material proportions associated with the

757 LGM suggest major shifts in site use or occupation associated with lowering sea levels (e.g.
758 Utting, 2017). There are no known outcrops of igneous rock in the general vicinity of Trảng
759 An, and various sources place the closest igneous outcrops between 50 and 80 km from the
760 landscape complex (Nguyen *et al.* 2012b, Tran, T.V., pers. comm).

761 *4.4 Sea level proxies in the RRD*

762 Conflicting chronologies for the Mid-Holocene transgression in the RRD from different
763 sediment cores as identified by Mann *et al.* (2019) can be resolved by considering notches in
764 Trảng An. Mann *et al.* (2019) report a difference between marker and index points of 20 m in
765 sea level around 10 ka BP and a discrepancy of 1000 years for the Mid-Holocene high stand
766 (Tanabe *et al.*, 2003a; Tanabe *et al.*, 2003b; Hori *et al.*, 2004). A subsequent paper by Tanabe
767 *et al.* (2006) presented further data from three cores from the southern coastal area of the
768 delta, which do not occur in the SEAMIS database. Contextualising and summarising the
769 various core data sets, they proposed a rsl of -40 m sometime after 11 – 12 ka BP based on
770 the fluvial/estuarine contact in ND-1. Whilst our survey cannot provide direct insight into sea
771 levels below modern mean sea level, a consideration of data from our notch surveys and from
772 Boyd and Lam (2004) is informative. Here we assume that sediments and geomorphological
773 markers in relatively close proximity to each other underwent similar vertical displacement
774 since the Mid-Holocene, with the south of the coastal RRD being uplifted while the north
775 subsided at a rate of 1 – 2mm pka for the past 20 years (Hai and Liem, 2011; Nguyen and
776 Takewaka, 2020). This rate, however, is unlikely to have been maintained over the last 5 – 7
777 ka and a comparison between contemporaneous sample sites from Hạ Long Bay and Trảng
778 An suggest a net vertical displacement of 0.5 (WK-8260/WK-8269) – 0.55 m (WK-
779 8255/WK-8267) since the Mid-Holocene. The upper bound may be reduced to 0.5 m if the
780 upper notch band of 5.6 m rsl from our survey is representative of the Mid-Holocene high

781 stand across the massif. A dedicated dating programme for notches in Trảng An and Hạ Long
782 Bay would reduce temporal ambiguity in the data sets and make them directly comparable.
783 As a whole, however, the notch data from Trảng An suggests that sea levels were still rising
784 at 7 ka BP, remaining significantly above modern sea level at around 6 ka BP rsl, and not
785 reaching present day sea level until at least 4 ka BP.

786 *4.5 Implications for modelling coastal vulnerability*

787 For over a decade, the Dynamic and Interactive Vulnerability Assessment (DIVA) model
788 (Hinkel and Klein, 2009), which was developed as part of the DINAS-COAST project, has
789 been particularly influential in predicting impacts from future sea level rise (e.g. Vafeidis et
790 al., 2008; Hinkel et al., 2014; Brown et al., 2016; Diaz, 2016; Muis et al., 2017; Tamura et
791 al., 2019). DIVA partitioned global coastlines (excluding Antarctica) into 12,148 linear
792 segments with uniform vulnerability to sea level rise and examined c. 80 different
793 biophysical and socio-economic parameters. This provision of semi-localised units of
794 assessment (median coastal segment: 18 km) with global coverage has been one of the
795 strengths of the approach, though it also inevitably introduces compromises; the potential
796 impact from two of these in particular is highlighted by the results of our study.
797 Coastal segments assessed through DIVA-based models, even when these are highly detailed
798 are constrained by a lack of time-depth. Future impact scenarios are extrapolated primarily
799 from a snapshot of current conditions with limited attention to the past. Deep-time records
800 such as those from Trảng An emphasise changes to coastal character (and hence potentially
801 also to segment classification), as well as the complexity of transgression and still-stand
802 episodes.
803 Our research also highlights the compromise that DIVA-based models make by excluding or
804 limiting changes to spatial structure (especially where these are also time-relative) in favour

805 of linear representations of the coastal zone. O'Donnell et al. (2020) demonstrated the
806 survival of mangrove forest elements within the Tràng An massif millennia after the Mid-
807 Holocene high stand had ended and the coastline had retreated. In this study, we have shown
808 how local conditions and specific hydromorphological features may have supported that
809 continuity. Coastal conditions need not be spatially confined to the linear transition zone
810 between terrestrial and marine environments that DIVA models track; nor do they necessarily
811 change in-step with changes to sea level.

812 The incorporation of a time-series and/or spatial structure into each defined coastal segment
813 is logistically and computationally impractical at a global scale, though it potentially holds
814 greater feasibility at a regional scale – as the recent Mediterranean study by Wolff et al.
815 (2018) demonstrates. We propose that targeted incorporation of anchor-point datasets that
816 utilise both dimensions, with particular reference to coastal areas of pronounced vulnerability to
817 sea level change, such as deltas, would be a valuable refinement to future regional models.

818 **5. Conclusions**

819 Detailed palaeo-coastline reconstruction for the Mid-Holocene marine transgression has been
820 carried out for the south-western extent of the RRD. The UNESCO World Heritage Site of
821 Tràng An stood at the centre of the investigation and modelling results have shown that
822 existing large-scale models underestimate the extent of the inundation in this area. Whilst
823 sufficient for regional and global coastal reconstructions, the error-margins attached to such
824 models potentially lead to misinterpretations of past human-landscape interactions.

825 Our current interpretation, supported by previous work (Lam and Boyd, 2001), places the
826 observed highest rsl at the Mid-Holocene high stand between 6 – 4 ka BP, turning Tràng An
827 into isolated near-shore archipelago. Under this scenario the central massif with its elevated
828 Pleistocene marine terrace constituted the only open plain within the archipelago that was

829 accessible from all contemporaneous archaeological sites. Hang Thung Bình and its five
830 principal caves stood in the centre of this plain. Mid-Holocene strata from its largest cave,
831 Hang Thung Bình 1, has only partially survived in excavated trenches but its advantageous
832 position in the landscape and its extensive use during the Pleistocene, makes this outcrop a
833 primary target for further investigation. This should certainly be extended to the plains
834 surrounding the hill in search for sites similar to the open-air Đa Bút sites that were found at
835 elevated terraces some 30 km southeast of Tràng An (Nguyen, 2005; Oxenham et al., 2018).
836 Finds here would extend the high density of archaeological sites from Early to Mid-Holocene
837 date, which are of considerable significance for Southeast Asian archaeology and the cultural
838 changes that took place at the Late-Pleistocene/ Early Holocene interface.
839 Our detailed study of notches as indicators for past rsl has established three, possibly four
840 discrete phases of stable sea levels above current mean sea level. These could indicate either
841 multiple transgressions or intermittent still-stands during transgression/ regression events and
842 highlight the complexity of sea level evolution.
843 In that context, we have clarified observed discrepancies between index and marker points
844 for water depth in existing palaeoecological reconstructions of the RRD and contributed a
845 new dataset that can be incorporated into the regional sea level curve. We have also
846 recommended that time-depth and spatial variability should be closely considered in the
847 preparation of future DIVA-based modelling in this and other regions. The research presented
848 here has demonstrated the potential importance of these dimensions not only to
849 archaeological reconstruction but also to modern coastal modelling and mitigation strategies.

850 **Funding**

851 This work was conducted as part of the SUNDASIA Project based at Queen's University
852 Belfast and principally funded by a UK Arts & Humanities Research Council (AHRC) Global

853 Challenges Research Fund (GCRF) grant (AH/N005902/1), a UK Research and Innovation
854 Covid-19 Grant Extension Allocation award and the Xuan Truong Construction Enterprise
855 (Vietnam).

856 **Author contributions**

857 **Thorsten Kahlert:** Conceptualisation, Methodology, Software, Investigation, Formal
858 analysis, Data curation, Visualisation, Writing – Original draft preparation, Review & Editing

859 **Shawn O'Donnell:** Conceptualisation, Methodology, Investigation – Vung Tham core,

860 Writing – Original draft preparation, Review & Editing **Christopher Stimpson:**

861 Conceptualisation, Investigation – Archaeological excavation director, Zooarchaeology,

862 Writing – Review & Editing **Nguyễn Thị Mai Hương:** Conceptualisation, Investigation –

863 TAK5 core, Writing – Review & Editing **Evan Hill:** Conceptualisation, Formal analysis –

864 Radiocarbon date calibration, Visualisation **Benjamin Utting:** Conceptualisation,

865 Methodology, Formal analysis, Writing – Original draft preparation, Review & Editing **Ryan**

866 **Rabett:** Conceptualisation, Methodology, Investigation, Writing – Original draft preparation,

867 Review & Editing, Supervision, Project Management, Funding acquisition, Resources

868 **Declaration of competing interest**

869 The authors declare that they have no competing interests that could have influenced the

870 work reported in this article.

871 **Acknowledgements**

872 The authors would like to thank the People's Committee of Ninh Bình, Mr. Nguyễn Văn

873 Trường and the Xuân Trường Enterprise for their ongoing support of the SUNDASIA

874 Project.

875 Field surveys were made with the support of Trảng An Management Board. Fieldwork could
876 not have been conducted without Vũ Duy Linh, Vũ Thùy Linh, Trương Thị Quỳnh Trang, Lê
877 Thị Thanh Kim Huệ, Vũ Thị Liên, Nguyễn Thị Loan, Phạm Sinh Khánh and Bùi Văn Mạnh.
878 Võ Thúy assisted in fieldwork, provided historic and archaeological expertise about Trảng
879 An.
880 Dr. Trần Tân Văn and Dr. Nguyễn Đại Trung of VIGMR supplied GIS data and their
881 expertise in the geology and geomorphology of Trảng An.
882 Nguyễn Thanh Long of VIGMR provided practical and logistical supported during our
883 survey of the national tidal benchmark at Hòn Đâu.
884 Phạm Anh Dũng of Tường Anh JSC supplied technical and material support.
885 Undergraduate students Kieran Kelly (QUB), Nguyễn Thu Hương (VNU) assisted in
886 fieldwork.
887 Corroborative field observations in Cát Bà Island were made possible by the generosity of the
888 Cát Bà Langur Conservation Project team: Neahga Leonard (Director), Mai Sỹ Luân, Phạm
889 Văn Tuyên, Lê Thị Ngọc Hân and Nguyễn Việt Anh.

890 **References**

- 891 Anderberg, M. R. 1973. *Cluster Analysis for Applications*. Academic Press.
892 <https://doi.org/10.1016/B978-0-12-057650-0.50012-0>.
- 893 Baker, R. G. V. & Haworth, R. J. 2000. Smooth or oscillating late Holocene sea-level curve?
894 Evidence from the palaeo-zoology of fixed biological indicators in east Australia and beyond.
895 *Marine Geology*, 163, 1, 367-86. [https://doi.org/10.1016/S0025-3227\(99\)00118-8](https://doi.org/10.1016/S0025-3227(99)00118-8).
- 896 Bird, M. I.; Austin, W. E. N.; Wurster, C. M.; Fifield, L. K.; Mojtahid, M. & Sargeant, C.
897 2010. Punctuated eustatic sea-level rise in the early mid-Holocene. *Geology*, 38, 9, 803-6.
898 <https://doi.org/10.1130/G31066.1>.

899 Boyd, W. & Lam, D. 2004. Holocene Elevated Sea Levels on the North Coast of Vietnam.
900 *Australian Geographical Studies*, 42, 77-88. <https://doi.org/10.1111/j.1467->
901 [8470.2004.00244.x](https://doi.org/10.1111/j.1467-8470.2004.00244.x).

902 Brock, G.; Pihur, V.; Datta, S. & Datta, S. 2008. clValid: An R Package for Cluster
903 Validation. *Journal of Statistical Software*, 25, 4, 1-22. <http://www.jstatsoft.org/v25/i04/>.

904 Brown, S.; Nicholls, R. J.; Lowe, J. A. & Hinkel, J. 2016. Spatial variations of sea-level rise
905 and impacts: An application of DIVA. *Climatic Change*, 134, 403-416.
906 <http://doi.org/10.1007/s10584-013-0925-y>.

907 Cerrano, C.; Azzini, F.; Bavestrello, G.; Calcinai, B.; Pansini, M.; Sarti, M. & Thung, D.
908 2006. Marine lakes of karst islands in Ha Long Bay (Vietnam). *Chemistry and Ecology*, 22,
909 6, 489-500. <https://doi.org/10.1080/02757540601024835>.

910 Diaz, D. B. 2016. Estimating global damages from sea level rise with the Coastal Impact and
911 Adaptation Model (CIAM). *Climatic Change*, 137, 143-156. <http://doi.org/10.1007/s10584->
912 [016-1675-4](http://doi.org/10.1007/s10584-016-1675-4).

913 Do, T.; Nguyen Dai, T.; Nguyen Dinh, H.; Dam, N.; Dinh Tien, D.; Tran Minh, T. & Trinh
914 Thi, T. 2012. The geological and tectonic character of Trang An, Ninh Binh. *Journal of*
915 *Geology*, 2013, 336, 8-22.

916 Dunn, J. C. 1974. Well-Separated Clusters and Optimal Fuzzy Partitions. *Journal of*
917 *Cybernetics*, 4, 1, 95-104. <https://doi.org/10.1080/01969727408546059>.

918 Fanchette, S. 2002. Le delta du Fleuve Rouge (Vietnam): étude des densités de population et
919 de l'urbanisation des campagnes. *Espace Populations Sociétés*, 1, 2, 189-202.
920 <https://doi.org/10.3406/espos.2002.2031>.

921 Funabiki, A.; Haruyama, S.; Quy, N. V.; Hai, P. V. & Thai, D. H. 2007. Holocene delta plain
922 development in the Song Hong (Red River) delta, Vietnam. *Journal of Asian Earth Sciences*,
923 30, 3, 518-29. <https://doi.org/10.1016/j.jseaes.2006.11.013>.

924 Galili, T. 2015. dendextend: an R package for visualizing, adjusting and comparing trees of
925 hierarchical clustering. *Bioinformatics*, 31, 22, 3718-3720.
926 <https://doi.org/10.1093/bioinformatics/btv428>.

- 927 Hai, V. & Liem, N. 2011. Determination of present crustal movements of Red River Fault
928 Zone by the TamDao - BaVi GPS network (1994-2007). *Vietnam Journal of Earth Sciences*,
929 33, 474-479.
- 930 Hanebuth, T.; Stattegger, K. & Grootes, P. M. 2000. Rapid Flooding of the Sunda Shelf: A
931 Late-Glacial Sea-Level Record. *Science*, 288, **5468**, 1033-1035.
- 932 Hanebuth, T.; Voris, H.; Yokoyama, Y.; Saito, Y. & Okuno, J. I. 2011. Formation and fate of
933 sedimentary depocentres on Southeast Asia's Sunda Shelf over the past sea-level cycle and
934 biogeographic implications. *Earth-Science Reviews*, 104, 92-110.
935 <https://doi.org/10.1016/j.earscirev.2010.09.006>.
- 936 Hanebuth, T. J. J.; Stattegger, K. & Bojanowski, A. 2009. Termination of the Last Glacial
937 Maximum sea-level lowstand: The Sunda-Shelf data revisited. *Global and Planetary Change*,
938 66, **1**, 76-84. <https://doi.org/10.1016/j.gloplacha.2008.03.011>.
- 939 Hens, L.; Thinh, N.; Hanh, T.; Cuong, N.; Tran Dinh, L.; Van Thanh, N. & Le, D. 2018. Sea-
940 level rise and resilience in Vietnam and the Asia-Pacific: A synthesis. *Vietnam Journal of*
941 *Earth Sciences*, 40, 127-153. <http://dx.doi.org/10.15625/0866-7187/40/2/11107>.
- 942 Hinkel, J. 2005. DIVA: An Iterative Method for Building Modular Integrated Models.
943 *Advances in Geosciences*, 4, 45–50. <http://doi.org/10.5194/adgeo-4-45-2005>.
- 944 Hinkel, J. & Klein, R. J. T. 2009. Integrating knowledge to assess coastal vulnerability to sea-
945 level rise: The development of the DIVA tool. *Global Environmental Change*, 19, 384-395.
946 <https://doi.org/10.1016/j.gloenvcha.2009.03.002>.
- 947 Hinkel, J.; Lincke, D.; Vafeidis, A. T.; Perrette, M.; Nicholls, R. J.; Tole, R. S. J.; Marzeiong,
948 B.; Fettweis, X.; Ionescu, C. & Levermann, A. 2014. Coastal flood damage and adaptation
949 costs under 21st century sea-level rise. *PNAS*, 111, **9**, 3292-3297.
950 <http://doi.org/10.1073/pnas.1222469111>.
- 951 Hinkel, J.; Nicholls, R.; Vafeidis, A.; Tol, R. & Avagianou, T. 2010. Assessing risk of and
952 adaptation to sea-level rise in the European Union: An application of DIVA. *Mitigation and*
953 *Adaptation Strategies for Global Change*, 15, 703-719. [http://doi.org/10.1007/s11027-010-](http://doi.org/10.1007/s11027-010-9237-y)
954 9237-y.

- 955 Hori, K.; Tanabe, S.; Saito, Y.; Haruyama, S.; Nguyen, V. & Kitamura, A. 2004. Delta
956 initiation and Holocene sea-level change: example from the Song Hong (Red River) delta,
957 Vietnam. *Sedimentary Geology*, 164, 3, 237-249.
958 <https://doi.org/10.1016/j.sedgeo.2003.10.008>.
- 959 Jones, R. K.; Piper, P. J.; Groves, C. P.; Nguyễn Anh, T.; Nguyễn Thi, M. H.; Nguyễn Thị,
960 H.; Hiep Hoang, T. & Oxenham, M. F. 2019. Shifting subsistence patterns from the Terminal
961 Pleistocene to Late Holocene: A regional Southeast Asian analysis. *Quaternary*
962 *International*, 529, 47-56. <https://doi.org/10.1016/j.quaint.2019.01.006>.
- 963 Kazmer, M.; Leman, M.; Mohamed, K.; Ali, C. & Taboroši, D. 2015. Features of Intertidal
964 Bioerosion and Bioconstruction on Limestone Coasts of Langkawi Islands, Malaysia. *Sains*
965 *Malaysiana*, 44, 921-929. <https://doi.org/10.17576/jsm-2015-4407-02>.
- 966 Kazmer, M. & Taborosi, D. 2012. Bioerosion on the small scale—examples from the tropical
967 and subtropical littoral. *Hantkeniana*, 7, 37-94.
- 968 Kelsey, H. M. 2015. Geomorphological indicators of past sea levels. In: Shennan, I.; Long,
969 A. J. & Horton, B. P. (eds.) *Handbook of Sea-Level Research*. Oxford: Wiley, 66-82.
970 <https://doi.org/10.1002/9781118452547.ch5>.
- 971 Kjerfve, B. 1994. Chapter 1 Coastal Lagoons. In: Kjerfve, B. (ed.) *Elsevier Oceanography*
972 *Series*. Elsevier, 1-8. [https://doi.org/10.1016/S0422-9894\(08\)70006-0](https://doi.org/10.1016/S0422-9894(08)70006-0).
- 973 Labbé, D. 2019. Examining the governance of emerging urban regions in Vietnam: the case
974 of the Red River Delta. *International Planning Studies*, 24, 1, 40-52.
975 <https://doi.org/10.1080/13563475.2018.1517593>.
- 976 Lam, D. & Boyd, W. 2001. Some facts of sea-level fluctuation during the late Pleistocene-
977 Holocene in Ha Long Bay and Ninh Binh area. *Journal of Sciences of the Earth*, 23, 86-91.
- 978 Lam, D. D. & Boyd, W. 2003. Holocene coastal stratigraphy and the sedimentary
979 development of the Hai Phong area of the Bac Bo Plain (Red River Delta), Vietnam.
980 *Australian Geographer*, 34, 2, 177-194. <https://doi.org/10.1080/00049180301737>.

981 Lambeck, K. 1990. Late pleistocene, holocene and present sea-levels: constraints on future
982 change. *Palaeogeography, Palaeoclimatology, Palaeoecology*, 89, 3, 205-217.
983 [https://doi.org/10.1016/0031-0182\(90\)90062-C](https://doi.org/10.1016/0031-0182(90)90062-C).

984 Lambeck, K. & Chappell, J. 2001. Sea level change through the last glacial cycle. *Science*,
985 292, 5517, 679-686. <https://doi.org/10.1126/science.1059549>.

986 Lap, N. V.; Ta, T. K. O. & Tateishi, M. 2000. Late Holocene depositional environments and
987 coastal evolution of the Mekong River Delta, Southern Vietnam. *Journal of Asian Earth*
988 *Sciences*, 18, 4, 427-439. [https://doi.org/10.1016/S1367-9120\(99\)00076-0](https://doi.org/10.1016/S1367-9120(99)00076-0).

989 Liew, P. M. & Hsieh, M. L. 2000. Late Holocene (2 ka) sea level, river discharge and climate
990 interrelationship in the Taiwan region. *Journal of Asian Earth Sciences*, 18, 4, 499-505.
991 [https://doi.org/10.1016/S1367-9120\(99\)00081-4](https://doi.org/10.1016/S1367-9120(99)00081-4).

992 Liew, P. M.; Pirazzoli, P. A.; Hsieh, M. L.; Arnold, M.; Barusseau, J. P.; Fontugne, M. &
993 Giresse, P. 1993. Holocene tectonic uplift deduced from elevated shorelines, eastern Coastal
994 Range of Taiwan. *Tectonophysics*, 222, 1, 55-68. [https://doi.org/10.1016/0040-](https://doi.org/10.1016/0040-1951(93)90189-Q)
995 [1951\(93\)90189-Q](https://doi.org/10.1016/0040-1951(93)90189-Q).

996 Maechler, M.; Rousseeuw, P.; Struyf, A.; Hubert, M. & Hornik, K. 2019. *cluster: Cluster*
997 *Analysis Basics and Extensions. R package version 2.1.0.*,

998 Mann, T.; Bender, M.; Lorscheid, T.; Stocchi, P.; Vacchi, M.; Switzer, A. D. & Rovere, A.
999 2019. Holocene sea levels in Southeast Asia, Maldives, India and Sri Lanka: The SEAMIS
1000 database. *Quaternary Science Reviews*, 219, 112-125.
1001 <https://doi.org/10.1016/j.quascirev.2019.07.007>.

1002 Mathers, S.; Davies, J.; McDonald, A.; Zalasiewicz, J. & Marsh, S. 1996. The Red River
1003 Delta of Vietnam. *British Geological Survey Technical Report WC/96/02*.

1004 Mathers, S. & Zalasiewicz, J. 1999. Holocene sedimentary architecture of the Red River
1005 Delta, Vietnam. *Journal of Coastal Research*, 2, 14, 314-325.

1006 McDonald, R. C. & Twidale, C. R. 2011. On the origin and significance of basal notches or
1007 footcaves in karst terrains. *Physical Geography*, 32, 3, 195-216.
1008 <https://doi.org/10.2747/0272-3646.32.3.195>.

- 1009 Metcalfe, I. 2017. Tectonic evolution of Sundaland. *Bulletin of the Geological Society of*
1010 *Malaysia*, 63, 27-60. <https://doi.org/10.7186/bgsm63201702>.
- 1011 Moses, C. A. 2012. Tropical rock coasts: Cliff, notch and platform erosion dynamics.
1012 *Progress in Physical Geography: Earth and Environment*, 37, 2, 206-226.
1013 <https://doi.org/10.1177/0309133312460073>.
- 1014 Muis, S.; Verlaan, M.; Nicholls, R. J.; Brown, S.; Hinkel, J.; Lincke, D.; Vafeidis, A. T.;
1015 Scussolini, P.; Winsemius, H. C. & Ward, P. J. 2017. A comparison of two global datasets of
1016 extreme sea levels and resulting flood exposure. *Earth's Future*, 5, 379-392.
1017 <http://doi.org/10.1002/2016EF000430>.
- 1018 Murray-Wallace, C. V.; Schnack, E. J. & (Eds.), J. O. 2003. IGCP Project 437: Coastal
1019 environmental change during sea-level highstands. *Marine Geology (Special Issue)*, 194, 1-2,
1020 1-134.
- 1021 Murray-Wallace, C. V. & Woodroffe, C. D. 2014. *Quaternary Sea-level Changes: A Global*
1022 *Perspective*. Cambridge: Cambridge University Press.
- 1023 Nguyen, D. T.; Tran, T. V.; Vu, V. H. & Trinh, T. T. 2012a. Sea levels and occupation of
1024 prehistoric people in karst valleys in Tràng An scenic complex (Ninh Bình). *Vietnam*
1025 *Archaeology*, 2012, 7, 13-23.
- 1026 Nguyen, G. D.; Nguyen, A. T. & Le, H. D. 2012b. Paleoenvironmental conditions and human
1027 adaptation in Trang An. *Vietnam Archaeology*, 7, 38-51.
- 1028 Nguyen, K. S. 2012. Tràng An cave archaeology outstanding cultural and historical values.
1029 *Vietnam Archaeology*, 2012, 7, 24-37.
- 1030 Nguyen, K. S. & Nguyen, A. T. 2012. Excavation at Vang rockshelter. *Vietnam Archaeology*,
1031 2012, 7, 81-93.
- 1032 Nguyen, Q. H. & Takewaka, S. 2020. Land subsidence and its effects on coastal erosion in
1033 the Nam Dinh Coast (Vietnam). *Continental Shelf Research*, 207, 104227.
1034 <https://doi.org/10.1016/j.csr.2020.104227>.
- 1035 Nguyen, V. 2005. The Da But culture: evidence for cultural development in Vietnam during
1036 the middle Holocene. *Bulletin of the Indo-Pacific Prehistory Association*, 25, 89-93.

- 1037 Nicholls, R. & Cazenave, A. 2010. Sea-level rise and its impact on coastal zones. *Science*,
1038 328, 1517-1520. <http://doi.org/10.1126/science.1185782>.
- 1039 Nielsen, L. H.; Mathiesen, A.; Bidstrup, T.; Vejbæk, O. V.; Dien, P. T. & Tiem, P. V. 1999.
1040 Modelling of hydrocarbon generation in the Cenozoic Song Hong Basin, Vietnam: a highly
1041 prospective basin. *Journal of Asian Earth Sciences*, 17, 1, 269-294.
1042 [https://doi.org/10.1016/S0743-9547\(98\)00063-4](https://doi.org/10.1016/S0743-9547(98)00063-4).
- 1043 Nishimura, M. & Phan, T. T. 2012. Preliminary results of excavation at Mòi Cave, Trảng An,
1044 Ninh Bình. *Vietnam Archaeology*, 2012, 7, 65-72.
- 1045 O'Donnell, S.; Nguyen, T. M. H.; Stimpson, C.; Holmes, R.; Kahlert, T.; Hill, E.; Vo, T. &
1046 Rabett, R. 2020. Holocene development and human use of mangroves and limestone forest at
1047 an ancient hong lagoon in the Trảng An karst, Ninh Binh, Vietnam. *Quaternary Science*
1048 *Reviews*, 242, 106416. <https://doi.org/10.1016/j.quascirev.2020.106416>.
- 1049 Omura, A.; Maeda, Y.; Kawana, T.; Siringan, F. P. & Berdin, R. D. 2004. U-series dates of
1050 Pleistocene corals and their implications to the paleo-sea levels and the vertical displacement
1051 in the Central Philippines. *Quaternary International*, 115-116, 3-13.
1052 [https://doi.org/10.1016/S1040-6182\(03\)00092-2](https://doi.org/10.1016/S1040-6182(03)00092-2).
- 1053 Oxenham, M.; Trinh, H.; Willis, A.; Jones, R.; Domett, K.; Castillo, C.; Wood, R.; Bellwood,
1054 P.; Tromp, M.; Kells, A.; Piper, P.; Pham, S.; Matsumura, H. & Buckley, H. 2018. Between
1055 foraging and farming: Strategic responses to the Holocene Thermal Maximum in Southeast
1056 Asia. *Antiquity*, 92, 940-957. <https://doi.org/10.15184/aqy.2018.69>.
- 1057 Pedoja, K.; Shen, J.-W.; Kershaw, S. & Tang, C. 2008. Coastal Quaternary morphologies on
1058 the northern coast of the South China Sea, China, and their implications for current tectonic
1059 models: A review and preliminary study. *Marine Geology*, 255, 3, 103-117.
1060 <https://doi.org/10.1016/j.margeo.2008.02.002>.
- 1061 Phach, P. V.; Lai, V. C.; Shakirov, R. B.; Le, D. A. & Tung, D. X. 2020. Tectonic Activities
1062 and Evolution of the Red River Delta (North Viet Nam) in the Holocene. *Geotectonics*, 54, 1,
1063 113-129. <https://doi.org/10.1134/S0016852120010094>.
- 1064 Pham, K. T.; Van, T. T.; Nguyen, D. T. & Nguyen, P. D. 2013. Geomorphology and
1065 outstanding landscape values of Trang An (Ninh Binh). *Vietnam Geology*, 2013, 36-49.

- 1066 Phan, L. 2014. *Late Pleistocene Lithic Technology at Hang Trống Cave, Vietnam: Climate*
1067 *Change and Hoabinhian Lithic Organization*. Unpublished MPhil dissertation, Department of
1068 Archaeology, University of Cambridge.
- 1069 Pirazzoli, P. A. 1986. Sea notches. In: Plassche, O. V. D. (ed.) *Sea-level Research: a Manual*
1070 *for the Collection and Evaluation of Data*. Norwich: Geo Books, 361-400.
- 1071 Pirazzoli, P. A. 1991. *World Atlas of Holocene Sea Level Changes*. Amsterdam: Elsevier.
- 1072 R Core Team 2018. *R: A language and environment for statistical computing*. Vienna,
1073 Austria: R Foundation for Statistical Computing.
- 1074 Rabett, R.; Appleby, J.; Blyth, A.; Farr, L.; Gallou, A.; Griffiths, T.; Hawkes, J.; Marcus, D.;
1075 Marlow, L.; Morley, M.; Tan, N. C.; Son, N. V.; Penkman, K.; Reynolds, T.; Stimpson, C. &
1076 Szabo, K. 2011. Inland shell midden site-formation: Investigation into a late Pleistocene to
1077 early Holocene midden from Trảng An, Northern Vietnam. *Quaternary International*, 239,
1078 1–2, 153-169. <http://dx.doi.org/10.1016/j.quaint.2010.01.025>.
- 1079 Rabett, R.; Barker, G.; Hunt, C. O.; Naruse, T.; Piper, P.; Raddatz, E.; Reynolds, T.; Van
1080 Son, N.; Stimpson, C.; Szabó, K.; Tân, N. C. a. O. & Wilson, J. 2009. The Trảng An Project:
1081 Late-to-Post-Pleistocene Settlement of the Lower Song Hong Valley, North Vietnam.
1082 *Journal of the Royal Asiatic Society of Great Britain & Ireland*, 19, 1, 83-109.
1083 <https://doi.org/10.1017/S1356186308009061>.
- 1084 Rabett, R.; Coward, F.; Tran, T. V.; Bui, V. M.; Strantzali, I. B.; Green, E.; Hill, E.; Holmes,
1085 R.; Kahlert, T.; Kelly, C.; Ludgate, N.; Macleod, R.; Mcallister, M.; Nguyen, C. T.; Nguyen,
1086 D. T.; Nguyen, T. H.; Nguyen, T. L.; Nguyen, T. M. H.; O'Donnell, S.; Pyne-O'Donnell, S.;
1087 Redmond, A.; Sinh, P. K.; Stimpson, C.; Tran, T. K. Q.; Truong, T. Q. T.; Utting, B.;
1088 Verhoeven, M.; Vu, D. L.; Vu, T. L. & Vu, T. L. 2019. Human Adaptation to Coastal
1089 Evolution: Late Quaternary evidence from Southeast Asia (SUNDASIA) –A report on the
1090 second year of the project. *Vietnam Archaeology*, 13, 23-48.
- 1091 Rabett, R.; Coward, F.; Van, T. T.; Manh, B. V.; Bachtsevanidou Strantzali, I.; Green, E. H.,
1092 E.; Holmes, R.; Kahlert, T.; Kelly, C.; Ludgate, N.; Macleod, R.; Magill, L.; Mcallister, M.;
1093 Trung, N. D.; Huong, N. T.; Loan, N. T.; Huong, N. T. M.; O'Donnell, S.; Von Oheimb, K.
1094 C. M.; Von Oheimb, P. V.; Redmond, A.; Khanh, S. P.; Stimpson, C.; Quy, T. T. K.; Son, T.

1095 V.; Thang, D. V.; Trang, T. T. Q.; Utting, B.; Verhoeven, M.; Linh, V. D.; Linh, V. T.; Lien,
1096 V. T. & Wilshaw, A. In review. Human adaptation to coastal evolution: Late quaternary
1097 evidence from Southeast Asia (SUNDASIA) – A report on the third year of the project.
1098 *Vietnam Archaeology*.

1099 Rabett, R.; Coward, F.; Van, T. T.; Stimpson, C. M.; Kahlert, T.; Bachtsevanidou; Strantzali,
1100 I.; Utting, B.; Trung, N. D.; Green, A.; Holmes, R.; Hue, L. T. T. K.; Lien, V. T.; Ludgate,
1101 N.; Linh, V. D.; Loyer, J.; Mann, D.; Dong, N. T.; Loan, N. T.; Khanh, P. S.; Son, P. T.;
1102 Simpson, D.; Quy, T. T. K.; Verhoeven, M.; Tan, N. C. & Manh, B. V. 2017a. Human
1103 Adaptation to Coastal Evolution: Late Quaternary evidence from Southeast Asia
1104 (SUNDASIA) – A report on the first year of the project. In: Unesco (ed.) *UNESCO 7B-*
1105 *VietNam-Trang An_20171206_public-1 Sub-Annex 1.1*.
1106 <http://whc.unesco.org/en/list/1438/documents/>,

1107 Rabett, R. & Jones, S. 2014. Post-glacial transformations in South and South-East Asia. In:
1108 Cummings, V.; Jordan, P. & Zvelebil, M. (eds.) *The Oxford Handbook of the Archaeology*
1109 *and Anthropology of Hunter-Gatherers*. Oxford: Oxford University Press, 492-506.

1110 Rabett, R.; Ludgate, N.; Stimpson, C.; Hill, E.; Hunt, C.; Ceron, J.; Farr, L.; Morley, M.;
1111 Reynolds, T.; Zulkwert, H.; Simpson, D.; Nyiri, B.; Verhoeven, M.; Appleby, J.; Meneely, J.;
1112 Phan, L.; Dong, N. N.; Lloyd-Smith, L.; Hawkes, J.; Blyth, A. & Tân, N. C. 2017b. Tropical
1113 limestone forest resilience and late Pleistocene foraging during MIS-2 in the Trảng An
1114 massif, Vietnam. *Quaternary International*, 448, 62-81.
1115 <http://dx.doi.org/10.1016/j.quaint.2016.06.010>.

1116 Ramsey, C. B. 2009. Bayesian analysis of radiocarbon dates. *Radiocarbon*, 51, 1, 337-360.

1117 Reimer, P. J.; Austin, W. E. N.; Bard, E.; Bayliss, A.; Blackwell, P. G.; Bronk Ramsey, C.;
1118 Butzin, M.; Cheng, H.; Edwards, R. L.; Friedrich, M.; Grootes, P. M.; Guilderson, T. P.;
1119 Hajdas, I.; Heaton, T. J.; Hogg, A. G.; Hughen, K. A.; Kromer, B.; Manning, S. W.;
1120 Muscheler, R.; Palmer, J. G.; Pearson, C.; Van Der Plicht, J.; Reimer, R. W.; Richards, D. A.;
1121 Scott, E. M.; Southon, J. R.; Turney, C. S. M.; Wacker, L.; Adolphi, F.; Büntgen, U.; Capano,
1122 M.; Fahrni, S. M.; Fogtmann-Schulz, A.; Friedrich, R.; Köhler, P.; Kudsk, S.; Miyake, F.;
1123 Olsen, J.; Reinig, F.; Sakamoto, M.; Sookdeo, A. & Talamo, S. 2020. The IntCal20 Northern
1124 Hemisphere Radiocarbon Age Calibration Curve (0–55 cal kBP). *Radiocarbon*, 62, 4, 725-
1125 757. 10.1017/RDC.2020.41.

- 1126 Reimer, P. J.; Bard, E.; Bayliss, A.; Beck, J. W.; Blackwell, P. G.; Ramsey, C. B.; Buck, C.
1127 E.; Cheng, H.; Edwards, R. L.; Friedrich, M.; Grootes, P. M.; Guilderson, T. P.; Haflidason,
1128 H.; Hajdas, I.; Hatté, C.; Heaton, T. J.; Hoffmann, D. L.; Hogg, A. G.; Hughen, K. A.; Kaiser,
1129 K. F.; Kromer, B.; Manning, S. W.; Niu, M.; Reimer, R. W.; Richards, D. A.; Scott, E. M.;
1130 Southon, J. R.; Staff, R. A.; Turney, C. S. M. & Van Der Plicht, J. 2016. IntCal13 and
1131 Marine13 Radiocarbon Age Calibration Curves 0–50,000 Years cal BP. *Radiocarbon*, 55, 4,
1132 1869-87. [10.2458/azu_js_rc.55.16947](https://doi.org/10.2458/azu_js_rc.55.16947).
- 1133 Reinecke, A. 2016. Das Paläolithikum bis zum Aufkommen von Keramik. In: Reinecke, A.
1134 (ed.) *Schätze der Archäologie Vietnams: Begleitband zur Sonderausstellung*. 2 ed. Mainz:
1135 Nünnerich-Asmus Verlag & Media, 42-68.
- 1136 Rovere, A.; Stocchi, P. & Vacchi, M. 2016. Eustatic and Relative Sea Level Changes.
1137 *Current Climate Change Reports*, 2, 4, 221-31. [10.1007/s40641-016-0045-7](https://doi.org/10.1007/s40641-016-0045-7).
- 1138 Scheffers, A.; Brill, D.; Kelletat, D.; Brückner, H.; Scheffers, S. & Fox, K. 2012. Holocene
1139 sea levels along the Andaman Sea coast of Thailand. *The Holocene*, 22, 10, 1169-1180.
1140 <https://doi.org/10.1177/0959683612441803>.
- 1141 Sloss, C. R.; Switzer, A. D.; Horton, B. P. & Zong, Y. E. 2012. Coastal Change during the
1142 Late Quaternary. *Quaternary Science Reviews (Special Issue)*, 54, 1-152.
- 1143 Small, C. & Nicholls, R. 2003. A global analysis of human settlement in coastal zones.
1144 *Journal of Coastal Research*, 19, 3, 584-599. <https://www.jstor.org/stable/4299200>.
- 1145 Stanley, D. J. & Warne, A. G. 1994. Worldwide initiation of Holocene marine deltas by
1146 deceleration of sea-level rise. *Science*, 265, 5169, 228.
1147 <https://doi.org/10.1126/science.265.5169.228>.
- 1148 Stanley, D. J. & Warne, A. G. 1997. Holocene sea-level change and early human utilization
1149 of deltas. *GSA Today*, 7, 12, 1-7.
- 1150 Stimpson, C. M.; Utting, B.; O'Donnell, S.; Huong, N. T. M.; Kahlert, T.; Manh, B. V.;
1151 Khanh, P. S. & Rabett, R. J. 2019. An 11 000-year-old giant muntjac subfossil from Northern
1152 Vietnam: implications for past and present populations. *Royal Society Open Science*, 6, 3,
1153 <https://doi.org/10.1098/rsos.181461>.

- 1154 Surakiatchai, P.; Choowong, M.; Charusiri, P.; Ch, T.; Chawchai, S.; Pailoplee, S.;
1155 Chabangborn, A.; Phantuwongraj, S.; Chutakositkanon, V.; Kongsen, S.; Nimnate, P. &
1156 Bissen, R. 2018. Paleogeographic reconstruction and history of the sea level change at Sam
1157 Roi Yot National Park, Gulf of Thailand. *Natural history*, 18, 112-34.
- 1158 Tamura, M.; Kumano, N.; Yotsukuri, M. & Yokoki, H. 2019. Global assessment of the
1159 effectiveness of adaptation in coastal areas based on RCP/SSP scenarios. *Climatic Change*,
1160 152, 363-377. <http://doi.org/10.1007/s10584-018-2356-2>.
- 1161 Tanabe, S.; Hori, K.; Saito, Y.; Haruyama, S.; Doanh, L. Q.; Sato, Y. & Hiraide, S. 2003a.
1162 Sedimentary facies and radiocarbon dates of the Nam Dinh-1 core from the Song Hong (Red
1163 River) delta, Vietnam. *Journal of Asian Earth Sciences*, 21, 5, 503-513.
1164 [https://doi.org/10.1016/S1367-9120\(02\)00082-2](https://doi.org/10.1016/S1367-9120(02)00082-2).
- 1165 Tanabe, S.; Hori, K.; Saito, Y.; Haruyama, S.; Vu, V. P. & Kitamura, A. 2003b. Song Hong
1166 (Red River) delta evolution related to millennium-scale Holocene sea-level changes.
1167 *Quaternary Science Reviews*, 22, 21, 2345-2361. [https://doi.org/10.1016/S0277-](https://doi.org/10.1016/S0277-3791(03)00138-0)
1168 3791(03)00138-0.
- 1169 Tanabe, S.; Saito, Y.; Lan Vu, Q.; Hanebuth, T. J. J.; Lan Ngo, Q. & Kitamura, A. 2006.
1170 Holocene evolution of the Song Hong (Red River) delta system, northern Vietnam.
1171 *Sedimentary Geology*, 187, 1, 29-61. <https://doi.org/10.1016/j.sedgeo.2005.12.004>.
- 1172 Tjia, H. D. 1996. Sea-level changes in the tectonically stable Malay-Thai Peninsula.
1173 *Quaternary International*, 31, 95-101. [https://doi.org/10.1016/1040-6182\(95\)00025-E](https://doi.org/10.1016/1040-6182(95)00025-E).
- 1174 Tran, T. V.; Nguyen, D. T.; Vu, V. H. & Trinh, T. T. 2013. Changing sea levels and the
1175 occupation by prehistoric people of karst valleys in the Trang An landscape complex, Ninh
1176 Binh. *Journal of Geology*, 2013, 336, 50-65.
- 1177 Trenhaile, A. 2016. Modelling coastal notch morphology and developmental history in the
1178 Mediterranean. *GeoResJ*, 9-12, 77-90. <https://doi.org/10.1016/j.grj.2016.09.003>.
- 1179 Trenhaile, A. S. 2015. Coastal notches: Their morphology, formation, and function. *Earth-*
1180 *Science Reviews*, 150, 285-304. <https://doi.org/10.1016/j.earscirev.2015.08.003>.

- 1181 Trenhaile, A. S. 2014. Modelling tidal notch formation by wetting and drying and salt
1182 weathering. *Geomorphology*, 224, 139-51. <https://doi.org/10.1016/j.geomorph.2014.07.014>.
- 1183 Tue, N. T.; Quan, D. M.; Nguyen, P. T.; Dung, L. V.; Quy, T. D. & Nhuan, M. T. 2018.
1184 Holocene environmental changes in Red River delta, Vietnam as inferred from the stable
1185 carbon isotopes and C/N ratios. *Journal of Earth System Science*, 128, 1, 15.
1186 <https://doi.org/10.1007/s12040-018-1041-1>.
- 1187 Unesco 2014a. Annex 3.3: Some results of Quaternary geological study of Trang An
1188 landscape complex. In: Unesco (ed.) *Nomination Document for the Inscription of the*
1189 *Properties on the List of World Heritage: Trang An Landscape Complex - Ninh Binh*
1190 *Province*. Paris,
- 1191 Unesco 2014b. *Trang An Landscape Complex, Ninh Binh, Vietnam*. UNESCO.
- 1192 Utting, B. 2017. *Exploring Prehistoric Behavioral Responses to Environmental Change at*
1193 *Tràng An, Ninh Binh Province, Vietnam*. Unpublished MPhil Dissertation, Department of
1194 Archaeology, University of Cambridge <https://doi.org/10.17863/CAM.12834>.
- 1195 Vafeidis, A. T.; Nicholls, R. J.; Mcfadden, L.; Tol, R. S. J.; Hinkel, J.; Spencer, T.; Grashoff,
1196 P. S.; Boot, G. & Klein, R. J. T. 2008. A new global coastal database for impact and
1197 vulnerability analysis to sea-level rise. *Journal of Coastal Research*, 24, 4, 917-924.
1198 <https://www.jstor.org/stable/40065185>.
- 1199 Waltham, T. 2009. Fengcong, fenglin, cone karst and tower karst. *Cave and Karst Science*,
1200 35, 3, 77-88.
- 1201 Wang, X. M.; Sun, X. J.; Wang, P. X. & Stattegger, K. 2008. The records of coastline
1202 changes reflected by mangroves on the Sunda Shelf since the last 40 ka. *Chinese Science*
1203 *Bulletin*, 53, 13, 2069-2076. <https://doi.org/10.1007/s11434-008-0278-5>.
- 1204 Wolff, C.; Vafeidis, A. T.; Muis, S.; Lincke, D.; Satta, A.; Lionello, P.; Jimenez, J. A.; Conte,
1205 D. & Hinkel, J. 2018. A Mediterranean coastal database for assessing the impacts of sea-level
1206 rise and associated hazards. *Nature: Scientific Data*, 5, 180044.
1207 <http://doi.org/10.1038/sdata.2018.44>.

- 1208 Woodroffe, S. A. & Horton, B. P. 2005. Holocene sea-level changes in the Indo-Pacific.
1209 *Journal of Asian Earth Sciences*, 25, 1, 29-43. <https://doi.org/10.1016/j.jseaes.2004.01.009>.
- 1210 Xie, Z.; Shao, H.; Chen, F.; Chen, Z. & Dou, Y. 1985. Transgression since Late Pleistocene
1211 in Fujian Coast. *International Geological Correlation Programme Project number 200 China*
1212 *working group*. Beijing: China Ocean Press.
- 1213 Yao, Y.; Harff, J.; Meyer, M. & Zhan, W. 2009. Reconstruction of paleocoastlines for the
1214 northwestern South China Sea since the Last Glacial Maximum. *Science in China Series D:*
1215 *Earth Sciences*, 52, 8, 1127-1136. <https://doi.org/10.1007/s11430-009-0098-8>.
- 1216 Zhang, Y.; Ma, Y.; Yang, N.; Shi, W. & Dong, S. 2003. Cenozoic extensional stress
1217 evolution in North China. *Journal of Geodynamics*, 36, 5, 591.

Accepted version